博士論文

Regulatory mechanisms of epidermal growth factor receptor signaling in cortical progenitor cells

（大脳皮質前駆細胞における上皮成長因子受容体シグナルの制御機構）

Izumi Fujimoto

Laboratory of Regulation of Neuronal Development
Institute for Protein Research
Osaka University

Table of Contents

SUMMARY

The growth factors EGF and bFGF are indispensable for maintaining the self-renewal and multipotency of neural stem cells residing in developing mammalian telencephalon. Cortical progenitor cells (CPCs) proliferate and differentiate into neuronal progenitors in response to bFGF at early stages of embryonic cortical development and into glial progenitors in response to EGF at the late stages. The EGF receptor (EGFR), a member of the receptor tyrosine kinase family, is expressed in the embryonic cortex, and its expression levels are low during the early period and high during the late period. EGFR promotes the differentiation and proliferation of astrocytes at late embryonic and neonatal stages of cortical development. Thus, the temporal and spatial differences in EGFR expression contribute to the fate diversification of CPCs by changing their responsiveness to EGF during normal cortical development. However, there is limited information about regulatory mechanisms of EGFR signaling in CPCs. Necdin is expressed abundantly in postmitotic neurons and moderately in CPCs. Necdin interacts with the NGF receptor TrkA, another receptor tyrosine kinase, to promote differentiation and survival of sensory neurons. Moreover, a study using yeast two-hybrid screening has identified necdin as one of the EGFR-interacting proteins. These findings prompted me to investigate the physical and functional interactions between EGFR and necdin in CPCs.

In the present study, I examined whether necdin interacts with EGFR in primary NPCs and controls gliogenesis. Primary NPCs were prepared from mice at embryonic day 14.5 and cultured in the presence of bFGF for 4 days. Immunocytochemical data showed that necdin was expressed in NPCs and co-localized with EGFR in the

cytoplasm after EGF treatment. Co-immunoprecipitation assay revealed that necdin bound to autophosphorylated EGFR but not to unphosphorylated EGFR. Necdin interacted directly with the tyrosine kinase domain (TKD) of EGFR, and deletion of the EGFR C-terminal domain enhanced the interaction, suggesting that the unphosphorylated C-terminal tail interferes with the interaction between necdin and the TKD. Necdin failed to affect EGF-dependent EGFR autophosphorylation in NPCs but reduced the interaction between EGFR and Grb2, an adaptor protein that activates the ERK1/2 pathway. In NPCs prepared from necdin-null mice, phosphorylated ERK1/2 levels were significantly increased. Furthermore, in necdin-null CPCs, astrocyte differentiation induced by the gliogenic cytokine cardiotrophin-1 was significantly accelerated in the presence of EGF, and inhibition of EGFR/ERK signaling abolished the acceleration. Moreover, necdin strongly suppressed astrocyte differentiation induced by overexpression of EGFR or its ligand binding-defective mutant equivalent to a glioblastoma-associated EGFR variant. These results suggest that necdin acts as an intrinsic suppressor of the EGFR/ERK signaling pathway in EGF-responsive CPCs to restrain astroglial development in a cell-autonomous manner.

PUBLICATION

Fujimoto, I., Hasegawa, K., Fujiwara, K., Yamada, M., and Yoshikawa, K.,
Necdin controls EGFR signaling linked to astrocyte differentiation in primary cortical progenitor cells, Cellular Signalling, **28**:94-107 (2016)

I. INTRODUCTION

I-1. General introduction

I-1-1. EGF and cortical development

In the 1950s, epidermal growth factor (EGF) was incidentally discovered by Stanley Cohen during the course of studies on the nerve growth factor. Since this discovery, a lot of biological effects of EGF have been found. In particular, EGF and basic fibroblast growth factor (bFGF, also known as FGF-2), another major growth factor, are indispensable for maintaining the self-renewal and multipotency of neural stem cells residing in developing mammalian telencephalon (Reynolds et al., 1992; Tropepe et al., 1999; Maric et al., 2003; Kilpatrick and Bartlett, 1995). Cortical progenitor cells (CPCs) change their responses to growth factors at different time points of development. CPCs proliferate and differentiate into neuronal progenitors in response to bFGF at early stages of embryonic cortical development and into glial progenitors in response to EGF at the late stages (Burrows et al., 1997; Qian et al., 2000; Lillien and Raphael, 2000; Sun et al., 2005). bFGF and EGF concentrations vary during development and CPCs respond differently to different concentrations of the same molecule (**Fig. I.1**). At the early stages, CPCs have no reactivity to EGF (Tropepe et al., 1999; Qian et al, 2000; Zhu and Parada, 2002; Gritti et al., 1999). As the stage progresses, the concentration of bFGF becomes high, leading to the induction of EGF receptor (EGFR) of CPCs (Qian et al., 1997; Powell et al., 1991). These temporal changes of CPCs in the responsiveness to EGF and bFGF are involved in the generation of specific cell types during cortical development (Temple, 2001).

I-1-2. EGFR and its signaling pathway

The EGF receptor (EGFR, also known as ErbB1/HER1) belongs to a receptor tyrosine kinase family, including ErbB2/Neu/HER2, ErbB3/HER3 and ErbB4/HER-4 (Schlessinger, 2002). The ligands for EGFR include EGF, transforming growth factor-alpha (Derynck et al., 1984), amphiregulin (Plowman et al., 1990), betacellulin (Sasada et al., 1993), heparin-binding EGF (Higashiyama et al., 1997), and epiregulin (Toyoda et al., 1997). Ligand binding to EGFR extracellular domain induces the formation of receptor homo- and heterodimers and the activation of the intrinsic protein tyrosine kinase domain (TKD), resulting in autophosphorylation on several tyrosine residues within the carboxy-terminal tail (Schlessinger, 2002; Yarden and Sliwkowski, 2001). Lysine (K) at the amino acid position 723 (K723) of EGFR is critical site for ATP binding activity and indispensable for EGFR autophosphorylation (Ewald et al., 2001). Autophosphorylated tyrosine (Y) residues act as specific binding sites for proteins containing Src-homology 2 (SH2) domains such as Grb2, Shc, and PLCγ. Phosphorylated EGFR interacts with the adaptor protein Grb2 at Y1068 and Y1086 (indirectly at Y1173 via Shc); Shc at Y994, Y1148, and Y1173; PLCγ at Y994, Y1086 and Y1173, the cytoplasmic tyrosine kinases Src and Abl at Y1086; the phosphatases PTP1B at Y994 and Y1148; and SHP-1 at Y1173 (Batzer et al., 1994; Novak et al., 2001; Sibilia et al., 2007). Y845 and Y1101 are phosphorylated by c-Src (Tice et al., 1999; Biscardi et al., 1999) (**Fig. I.2**). The major downstream signaling pathways regulated by EGFR are Ras-Raf-MEK-ERK1/2 pathway that mainly regulates proliferation and differentiation and the PI3K-Akt-mTOR cascade that acts as pro-survival and anti-apoptotic pathways (Yarden and Sliwkowski, 2001; Batzer et al., 1994; Sibilia et al., 2007) (**Fig. I.3**).

I-1-3. Negative feedback regulation of EGFR signaling

The attenuation of these signaling pathways is essential to maintain the signaling homeostasis. Termination of EGFR signaling occurs via endocytosis and lysosomal degradation, which are in part regulated by ligand-induced multiple EGFR monoubiquitylation, but not polyubiquitylation (Dikic and Giordano, 2003; Haglund et al., 2003; Mosesson et al., 2003). Cbl, a ubiquitin ligase for EGFR, is recruited to phosphorylated EGFR at the plasma membrane, and remains associated with activated EGFR throughout the endosomal compartment (de Melker et al., 2001). EGFR ubiquitination, which is regulated in a ligand concentration-dependent manner, correlates with the differential recruitment of EGFR into distinct endocytic pathways (Woelk et al. 2006; Acconcia et al., 2009). At low EGF concentrations, EGFR is almost exclusively internalized through the clathrin-dependent pathway without ubiquitination. At higher EGF concentrations, a substantial fraction of EGFR is endocytosed through a clathrin-independent, lipid raft-dependent pathway, and undergoes ubiquitination (Sigismund et al., 2005). Endocytosis ultimately leads to the extinction of the EGFR activity through degradation of ligand-receptor complexes in the lysosome.

I-1-4. EGFR singling-inducible feedback inhibitors

In mammalian cells, four EGFR inducible feedback inhibitors (IFIs) LRIG1, MIG6 (also known as RALT and ERRFI1), SOCS4 and SOCS5 have been reported to date (Segatto et al., 2011). All EGFR IFIs bind to EGFR directly to suppress the receptor signaling. LRIG1 binds to the extracellular region of the EGFR in a ligand-independent manner and promotes ligand-dependent ubiquitination of EGFR (Gur et al., 2004). SOCS4 and SOCS5, which includes an SH2 domain, bind to the EGFR in a

ligand-independent fashion (Kario et al., 2005; Nicholson et al., 2005). However it remains unclear how the SH2 domain of SOCS4 and SOCS5 is recruited to the EGFR in the absence of ligand-induced receptor tyrosine phosphorylation. The inhibition of EGFR signaling by SOCS4 and SOCS5 might be accomplished upon EGFR ubiquitination in both active and inactive states by an unidentified E3 ligase that is recruited to the SOCS-box-bound elongins B and C, subunits of the transcription factor B complex (Kario et al., 2005; Segatto et al., 2011). MIG6 binds to ligand-activated EGFR TKD and inhibits downstream EGFR signaling, including the Ras-Raf-MEK-ERK1/2 and the PI3K-Akt-mTOR pathways (Anastasi et al., 2003; Zhan et al., 2007). MIG6-bound EGFR is endocytosed and eventually degraded at the lysosome (Frosi et al., 2010; Madshus and Stang, 2009).

I-1-5. Inactive and active states of EGFR

Activation of the TKD of EGFR is controlled primarily by allosteric interactions between two TKDs; the TKD of one receptor molecule (the activator) activates the TKD of a second receptor (the receiver)(Zhang et al., 2006; Jura et al., 2009). The EGFR TKD is consist of N-terminal lobe (N-lobe) and C-terminal lobe (C-lobe) (**Fig.1.4A**). The TKD exhibits marked conformational changes when activated or mutated. The smaller N-lobe, largely constituted by β-sheet and the highly conserved C helix, contributes predominantly to the conformational change of the ATP-binding pocket (**Fig. I.4B**). The C-lobe, which is larger than the N-lobe, is mostly helical. ATP binds to the deep cleft between the lobes located near a highly conserved N-lobe structure known as the phosphate-binding loop (P-loop), which contains a conserved glycine-rich/sequence motif (GXGXφG). The kinases take two conformations in active

and inactive states (**Fig. I.4B**). The activation loop (A-loop), which is phosphorylated in the active state, serves as a platform (Nie et al., 2012).

I-1-6. EGFR and cancers

In numerous cancers such as glioblastoma, breast cancer, and non-small-cell lung cancer (NSCLC), there is often a transforming deregulation of EGFR signal transduction (Sibilia et al., 2007). Although several EGFR mutations have been described, the most common extracellular mutation is EGFRvIII (also known as de2-7EGFR). EGFRvIII is a tumor-specific mutation that results from in-frame deletion of 801 base pairs spanning exons 2-7 encoding the protein-coding sequence (Jungbluth et al., 2003; Voldborg et al., 1997; Wikstrand et al., 1995). This deletion removes 267 amino acids from the extracellular domain, creating a junction site between exon 1 and 8 (Yamazaki et al., 1990; Humphrey et al., 1988). Single point mutations in exon 21, for example L858R and G719S, account for approximately 50% of EGFR-TKD activating mutations (Kumar et al., 2008). Therefore, EGFR have been intensely pursed as therapeutic targets (Holbro and Hynes, 2004). The small-molecule gefitinib (Iressa) is the first EGFR-targeted inhibitor that received approval for the treatment of NSCLC. To date, several antibodies directed against the extracellular domain of EGFR and tyrosine kinase inhibitors (TKIs) that suppress the activity of the EGFR TKD are in clinical use or at advanced developmental stages. The treatment of tumor cells with these agents affects many of the intracellular pathways essential for cancer development and progression (Hynes and Lane, 2005).

I-2. Specific Introduction

I-2-1. Necdin and MAGE family

Necdin (Neurally differentiated embryonal carcinoma derived protein) was originally identified from a subtraction cDNA library of neurally differentiated P19 embryonal carcinoma cells (Maruyama et al., 1991). Necdin is a 325-amino acids residues protein, containing highly acidic and proline-rich regions at the N-terminal regions (1-100 amino acids) and MAGE homology domain (MHD) at rest of regions (101-325 amino acids) (Taniura et al., 1998). Necdin is belongs to the MAGE (melanoma antigen) family protein. A group of MAGE genes such as MAGE-A, B, and C are classified as Type I MAGE proteins expressed in cancer and germ cells. In contrast, Type II MAGE proteins including necdin, MAGE-D, E, F, G, and H are expressed in normal cells and tissues (Barker and Salehi, 2002). In fact, Necdin is expressed abundantly in postmitotic neurons and moderately in neural precursor cells (Uetsuki et al., 1996; Huang et al., 2013; Minamide et al., 2014). Necdin is also expressed in non-neuronal cells such as skeletal and smooth muscle, chondrocytes, adipocytes, and skin fibroblasts (Gérard et al., 1999; Yoshikawa, 2000; Hu et al., 2003; Brunelli et al., 2004; Kuwajima et al., 2004; Fujiwara et al., 2012). It is noteworthy that necdin is preferentially expressed in postmitotic neurons and non-neuronal cells. Ectopic expression of necdin strongly suppresses the proliferation of many cell lines such as NIH3T3 cells, osteosarcoma SAOS-2 cell, and N1E-115 neuroblastoma cells (Hayashi et al., 1995; Taniura et al., 1999; Kobayashi et al., 2002).

I-2-2. Biological function of necdin

The biological functions and molecular mechanisms have been elucidated through

identification of necdin binding proteins. Necdin interacts with cell cycle regulatory transcripton factors E2Fs, p53, Msx, and HIF-2α to suppress transcriptional activation and cell cycle progression (Taniura et al., 1998; Huang et al., 2013; Kuwajima et al., 2004; Kobayashi et al., 2002; Taniura et al., 1999). Necdin also interacts with $p75^{NTR}$, TrkA, Dlx, and Sirt1 to promote neuronal differentiation and survival or to suppress apoptosis (Kuwako et al., 2004; Kuwako et al., 2005; Hasegawa and Yoshikawa 2008; Hasegawa et al., 2012). In addition, the calcium-binding protein NEFA, hnRNP-U (heterogenous nuclear ribonucleoprotein U), SV40 large T antigen, adenovirus E1A, Fez1, Bmi1, and PIAS1 have been identified as necdin-binding proteins (Minamide et al., 2014; Taniguchi et al., 2000; Taniura and Yoshikawa 2002; Lee et al., 2005; Gur et al., 2014). Thus, necdin have diverse functions through association with proteins which regulate the cell cycle, apoptosis and differentiation in the nervous system and non-neuronal tissues.

Necdin interacts with the NGF receptor TrkA, a receptor tyrosine kinase (Kuwako et al., 2005). Moreover, a study using yeast two-hybrid screening has identified necdin as one of the EGFR-interacting proteins (Deribe et al., 2009). These findings led us to investigate the physical and functional interactions between EGFR and necdin in CPCs.

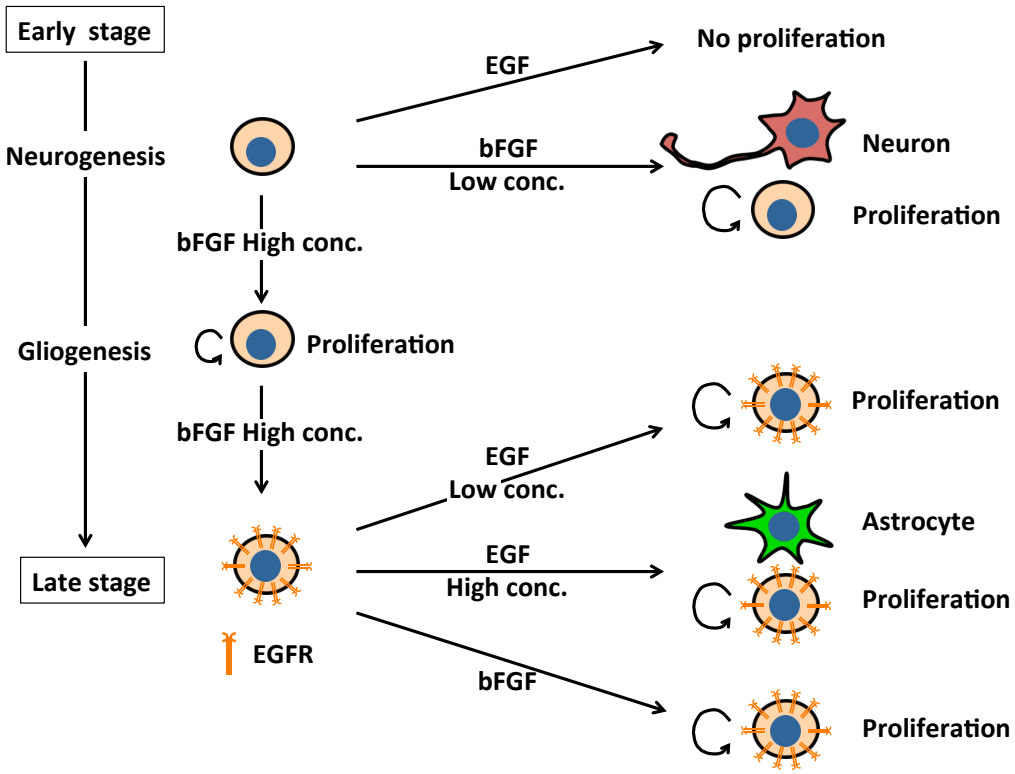

Figure I.1 Neurogenesis and gliogenesis during cortical development.
CPCs alter their responses to growth factors at different stages of corticogenesis (adapted from Temple S, 2001).

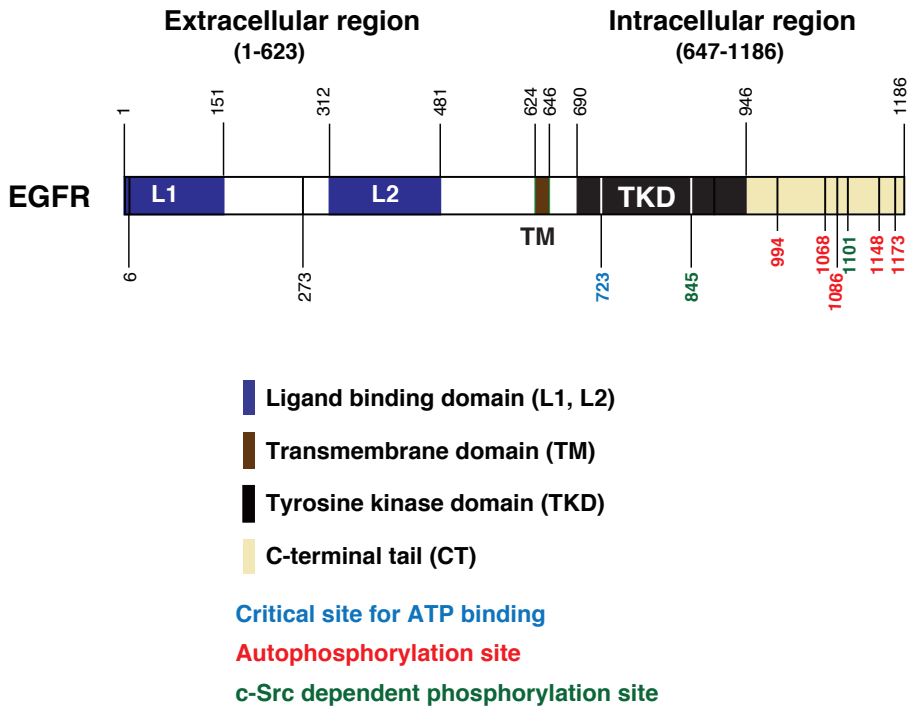

Figure I.2 Domain structure of mouse EGFR.
Sequence information was obtained from NCBI NM 207655.2.

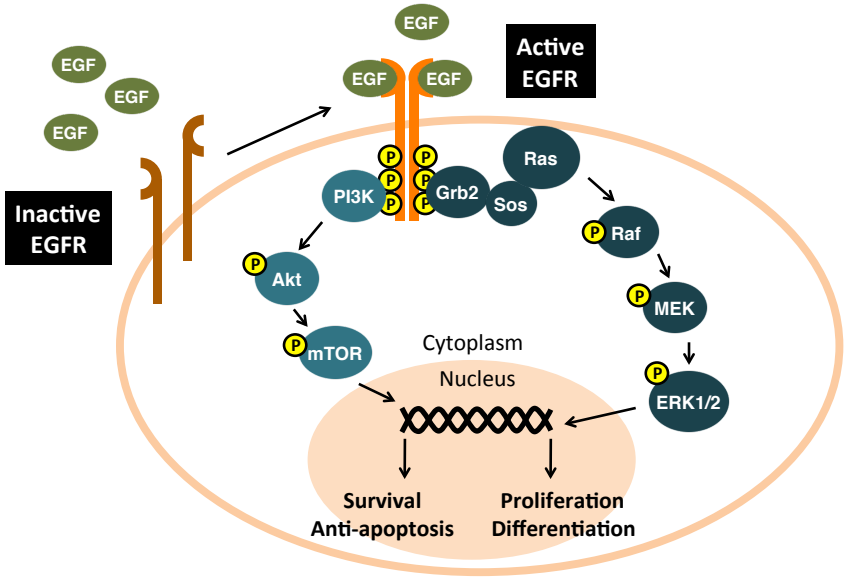

Figure I.3 EGFR signaling pathway.
The Ras-Raf-MEK-ERK1/2 pathway mainly regulates proliferation and differentiation, while the PI3K-Akt-mTOR pathway mainly regulates survival and apoptosis.

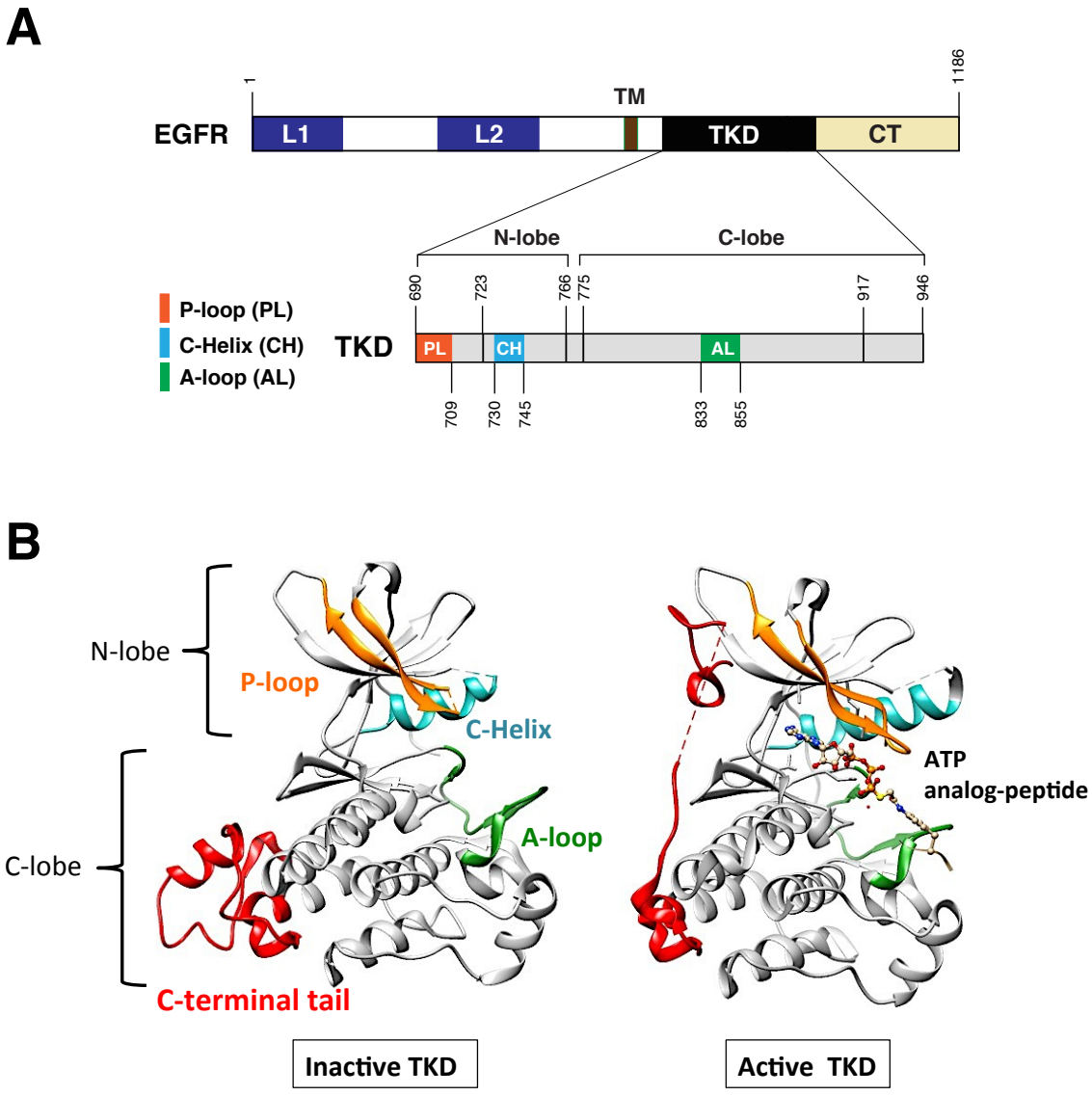

Figure I.4 Ribbon representation of the two crystalized conformations of EGFR TKD.

(**A**) Primary structure of EGFR TKD. Sequence information was obtained from NCBI NM 207655.2. L1/2, ligand-biding domain 1/2; TM, transmembrane domain; CT, C-terminal tail. (**B**) Crystal structures of inactive EGFR TKD (PDB 4G5J)(left) and active EGFR TKD in complex with ATP analog-peptide (PDB 2GS6)(right).

II. EXPERIMENTAL PROCEDUES

II-1. Primary cortical progenitor cells

Neocortical tissues were dissected from mouse embryos at embryonic day (E) 14.5, incubated for 5 min at 37°C in Ca^{2+}/Mg^{2+}-free glucose-supplemented HBSS with 0.05% trypsin, dissociated in DMEM supplemented with 10% fetal bovine serum, and centrifuged at 200 × g for 3 min to obtain cell pellets. Resuspended cells were incubated at 37°C under humidified 5% CO_2 conditions in CPC medium containing DMEM/F12 (Thermo Fisher Scientific), B-27 (1:50 dilution; Thermo Fisher Scientific), 14 mM sodium bicarbonate, 1 mM N-acetyl-L cysteine, 33 mM D (+)-glucose, 1 mg/ml bovine serum albumin, 2 mM GlutaMAX (Thermo Fisher Scientific), kanamycin/penicillin, and 20 ng/ml bFGF (PeproTech). CPCs were grown as floating spheres, dispersed with TrypLE (TrypLE Select; Thermo Fisher Scientific), and passaged every 48 h unless stated otherwise. Necdin gene (*Ndn*) mutant mice were generated and maintained as described previously (Kuwako et al., 2005). Heterozygous male mice ($Ndn^{+/-}$)(>25 generations in the ICR background) were crossed with wild-type female mice ($Ndn^{+/+}$)(Japan SLC) to obtain wild-type ($Ndn^{+m/+p}$) and paternal *Ndn*-deficient ($Ndn^{+m/-p}$) littermates. All mice were housed in a 12 h light/dark cycle with room temperature at 23 ± 3°C. Pregnant female mice at gestation day 14.5 were sacrificed by cervical dislocation, and embryos were collected. Genotypes of all mice were analyzed for mutated *Ndn* locus. The study was approved by the Animal Experiment Committee (Approval No. 24-04-0) and Recombinant DNA Committee (Approval No. 3642) of Institute for Protein Research, Osaka University, and were performed in accordance

with national, institutional, and the ARRIVE guidelines.

II-2. Immunoblot analysis

CPCs and brain tissues were homogenized with a lysis buffer containing 10 mM Tris-HCl (pH 8.0), 150 mM NaCl, 1 mM EDTA, 1% IGEPAL CA-630 (MP Biomedicals), 10% glycerol, and protease inhibitors (Complete, Roche Diagnostics). The protein concentration was determined by the Bradford method (Bio-Rad). Proteins (10 μg per lane) were separated by 9% SDS-PAGE, and electroblotted to polyvinylidene difluoride membranes (Immobilon, Merck Millipore). Membranes were incubated with primary antibodies against EGFR (1005; 1:100; Santa Cruz Biotechnology), necdin (NC243; 1:3000)(Niinobe et al., 2000), nestin (ST-1; 1:1000)(Aizawa et al., 2011), γ-tubulin (GTU-88; 1:1000; Sigma-Aldrich), phospho-EGFR (Tyr1068)(D7A5; 1:1000; Cell Signaling Technology), PCNA (PC10; 1:1000; Santa Cruz Biotechnology), Myc (9E10; 1:10), phospho-ERK1/2 (E10; 1:1000; Cell Signaling Technology), ERK1/2 (K-23; 1:3000; Santa Cruz Biotechnology), phospho-Akt (193H12; 1:500; Cell Signaling Technology), Akt (1:500; Cell Signaling Technology), Grb2 (C-7; 1:300; Santa Cruz Biotechnology), Sos1 (C-23; 1:1000; Santa Cruz Biotechnology), glial fibrillary acidic protein (GFAP)(1:1000; gift from Dr. Seiichi Haga, Tokyo Metropolitan Institute of Medical Science), and FLAG (M2; 1:500; Sigma-Aldrich),. After incubation with peroxidase-conjugated IgGs (Cappel), the proteins were visualized by chemiluminescence method (Chemiluminescence Reagent Plus, PerkinElmer). Signal intensities were measured by densitometry and quantified using NIH ImageJ 1.46 software.

II-3. Immunocytochemistry

Primary CPCs were dispersed with TrypLE Select, plated onto 24-well plates precoated with poly-L-ornithine (Sigma-Aldrich), and incubated for 3 h. Cells were fixed with 10 % formalin solution at room temperature for 20 min and permeabilized with methanol at room temperature for 20 min. For EGFR staining, cells were fixed with 4% paraformaldehyde in phosphate buffer (pH 7.4) and permeabilized with 0.02% Tween 20 in PBS at room temperature for 10 min. Fixed cells were incubated with primary antibodies at 4°C overnight, and with secondary antibodies at room temperature for 90 min. The primary antibodies used are against EGFR (1005; 1:50), necdin (GN1; 1:1000)(Kuwako et al., 2005), nestin (ST-1; 1:1000), phospho-EGFR (D7A5; 1:100), GFAP (1:1000), βIII-tubulin (5G8; 1:1000; Promega), and RFP (3G5, 1:100, MBL). The secondary antibodies Alexa 488-conjugated anti-rabbit IgG (1:500), Alexa 555-conjugated anti-guinea pig IgG (1:500), and Alexa 555-conjugated anti-rabbit IgG (1:500) were purchased from Molecular Probes. Nuclear DNA was counterstained with 3.3 μM Hoechst 33342 (Sigma-Aldrich). Images were observed with a fluorescence microscope (BX51, Olympus) equipped with charge-coupled device camera system (DP73, Olympus) or by confocal laser scanning microscopy (FV1000 BX61, Olympus), and processed using Adobe Photoshop CS5 software.

II-4. Coimmunoprecipitation assay

For detection of endogenous binding between necdin and EGFR, lysates of CPCs (1 mg protein) cultured in the CPC medium for 4 days were incubated with guinea pig anti-necdin IgG (GN1; 1:10)(Kuwako et al., 2005) or preimmune IgG. Bound proteins were isolated with Dynabeads protein A (Thermo Fisher Scientific) and detected by

immunoblotting with antibodies against phospho-EGFR (D7A5; 1:1000), EGFR (1005; 1:100) and necdin (NC243; 1:3000). For interactions between necdin and EGFR mutants in transfected cells, HEK293A cells were transfected with combinations of expression vectors by the calcium phosphate method and harvested after 24 h. Cell lysates (150 μg protein) were incubated at 4°C for 2 h with antibodies against Myc (9E10; 1:4) and necdin (NC243; 1:100), pelleted with Protein A-Sepharose (GE Healthcare), separated by 9% SDS-PAGE, and detected by immunoblotting. Full-length mouse EGFR cDNA (NCBI NM 207655.2) was synthesized by RT-PCR from mRNA expressed in CPCs. cDNAs encoding EGFR deletion mutants and its point mutants were generated using synthetic oligonucleotide primers based on their sequence information (NCBI NM 207655.2) and subcloned into 6xMyc-pcDNA3.1+. For interactions of EGFR with Grb2 and Sos1, primary CPCs prepared from E14.5 mice were cultured for 4 days and treated with EGF (10 ng/ml) for 5 min. CPC lysates (500 μg protein) were incubated with antibodies to Grb2 (C-7; 1:100) and Sos1 (C-23; 1:100). Bound proteins were pelleted with Protein A-Sepharose and detected by immunoblotting with the antibody to EGFR (1005; 1:100).

II-5. In vitro binding assay

The tyrosine kinase domain (TKD) of EGFR and its deletion mutants were generated using synthetic oligonucleotide primers based on their sequence information (NCBI NM 207655.2) and subcloned into pMAL-C2 vector to make maltose binding protein (MBP) fusion proteins. MBP-fused proteins were affinity-purified with amylose resin (New England Biolabs) and incubated with His-tagged necdin (200 ng) at 4°C for 30 min in 0.5 ml of the binding buffer containing 20 mM Tris-HCl (pH7.5), 200 mM

NaCl, and 1 mM EDTA (Hasegawa and Yoshikawa, 2008). After washing, bound His-tagged necdin was eluted with 20 mM maltose and detected by immunoblotting with anti-necdin antibody. MBP fusion proteins were detected by Coomassie Brilliant Blue staining.

II-6. Cell proliferation assay

Primary CPCs were prepared from E14.5 mice and incubated for 48 h. Cells (2 x 10^5 cells) were replated in 35-mm dishes, incubated in the presence or absence of 20 ng/ml EGF for another 48 h, and harvested for manual cell counting. For EdU incorporation, CPCs at 4 day *in vitro* (DIV) were plated onto poly-L-ornithine-coated coverslips. Cells were cultured in the CPC medium supplemented with 10 ng/ml EGF for 24 h and fixed with 10% formalin solution at room temperature for 20 min, and permeabilized with methanol at room temperature for 20 min. EdU (Invitrogen, A10044; 10 μM) was added to the CPC medium 4 h before fixation. Fixed cells were incubated for 30 min with 3.3 μM Hoechst 33342 (Sigma-Aldrich) and then with EdU detection cocktail (A10044, Invitrogen) at room temperature for 15 min.

II-7. Cell differentiation assay

For astrocyte differentiation assay, CPCs cultured for 48 h in the CPC medium were incubated in the presence and absence of 20 ng/ml EGF for 48 h. CPCs were dissociated and plated onto poly-L-ornithine-coated coverslips in the CPC medium supplemented with 50 ng/ml cardiotrophin-1 (CT-1)(PeproTech) for 48 h. GFAP-immunopositive cells were detected by immunocytochemistry as above. For neuronal differentiation assay, CPCs cultured for 48 h in the CPC medium were

incubated in the presence and absence of 20 ng/ml EGF for 48 h. CPCs were dissociated, plated onto poly-L-ornithine-coated coverslips and cultured in the CPC medium deprived of EGF and bFGF for 24 h. βIII tubulin-expressing cells were detected by immunocytochemistry as above.

II-8. Kinase inhibitor assay

CPCs were cultured in the CPC medium for 48 h, and EGF (10 ng/ml) in the presence of the EGFR tyrosine kinase inhibitor gefitinib (5 μM; Cayman Chemical), mitogen-activated protein kinase kinase (MEK) inhibitor U0126 (20 μM; Merck Millipore) and phosphoinositide 3-kinase (PI3K) inhibitor LY294002 (20 μM; Merck Millipore) were added to the CPC medium 30 min before treatment with EGF. CPCs were treated with EGF (10 ng/ml) for 5 min and harvested for immunoblot analysis of phospho-EGFR, phospho-ERK, and phospho-Akt. For GFAP expression assay, CPCs were treated with EGF and the kinase inhibitors for 6 h, replated in 35-mm dish precoated with poly-L-ornithine, and treated with CT-1 (50 ng/ml) for 48 h. Expression of GFAP was analyzed by immunoblotting.

II-9. In vitro electroporation.

CPCs were prepared from E14.5 mice and cultured for 48 h. CPCs were centrifuged and resuspended at 5 x 10^6 cells in 100 μl of Opti-MEM containing expression vectors (total DNA, 20 μg). Electric pulses (pore pulse; 125V/10 msec x 1: transfer pulse; 20V/50 msec/50 msec interval; 10 cycles) were applied to the cell suspension in 2-mm gap cuvette using a pulse generator (CUY21-EDIT II, BEX).

cDNA encoding EGFR lacking residues 6-273 (EGFRΔNT) was generated using synthetic oligonucleotide primers based on their sequence information (NCBI NM 207655.2) and subcloned into 6xMyc-pcDNA3.1+. cDNAs for EGFR, EGFR mutants (KR and ΔNT), FLAG-tagged mouse necdin, necdinΔEB (residues 144-184 deletion mutant)(Taniura et al., 2005), FLAG-tagged human MAGEA1(Gur et al., 2014), and td-Tomato (ptdTomato-N1, Clontech) were transfected into primary CPCs. Transfection efficiency was ~70% as analyzed 12 h after transfection by fluorescence immunocytochemistry for td-Tomato expression. Expression of transfected cDNAs was analyzed by immunoblotting 12 h after electroporation. For GFAP expression, transfected CPCs were cultured for 24 h in the CPC medium and treated with CT-1 (50 ng/ml) for 48 h. GFAP expression of transfected CPCs was analyzed by immunoblotting and fluorescence immunocytochemistry using antibodies to GFAP and RFP for td-Tomato.

II-10. Quantitative RT-PCR

Total RNA was extracted with phenol and guanidine thiocyanate mixture (TRI Reagent, Molecular Research Center), and contaminating DNA was digested with RQ1 RNase-free DNAase (Promega). cDNA was synthesized from total RNA (2 μg) using Transcriptor First Strand cDNA Synthesis Kit (Roche Diagnostics). An aliquot of cDNA mixture (0.2%) was used as PCR templates. Primers used for quantitative real-time PCR are as follows: EGF (forward, 5’-caagtgatggatagacgtga-3’; reverse, 5’-cagggatggataacggttag-3’), Gapdh (forward, 5’-gaatacggctacagcaa-3’; reverse, 5’-gcagcgaactttattgatggta-3’), cFOS (forward, 5’-agttagtagagcatgtgagt-3’; reverse, 5’-tgaaggactacagtacatgg-3’), cJUN (forward, 5’-ttgtaagtgccaggctagac-3’; reverse,

5’-catgcagggtatctattccaca-3’), EGR1 (forward, 5’-catgtgtcagagtgttgttccgt-3’; reverse, 5’-agcgcattcaatgtgtttataagcc-3’), EGR2 (forward, 5’-tcaagagaatggaagtgcaa-3’; reverse, 5’-gccatacttaaacccaagga-3’), IEX1 (forward, 5’-gcttttctccagcaacatcc-3’; reverse, 5’-ttacatacacccctccttcac-3’). RT-PCR products were quantified using FastStart DNA MasterPLUS SYBR Green I kit (Roche Diagnostics). Melting curves were analyzed to confirm a single species of each PCR product. Gapdh cDNA was used as an internal control to quantify the relative expression of each cDNA.

II-11. Statistics

Statistical significance was tested using an unpaired Student’s *t* test, one-way ANOVA followed by Tukey-Kramer *post hoc* test. A significance of $P < 0.05$ was required for rejection of the null hypothesis.

III. RESULTS

III-1. EGFR expression is induced by bFGF in primary CPCs

We first analyzed the expression levels of EGFR and necdin in primary CPCs prepared from the mouse cortex at E14.5 by immunoblotting (**Fig. III.1A**). When CPCs were treated with bFGF for up to 4 DIV, the EGFR levels increased when incubated in the presence of bFGF for 2 days or more, whereas necdin was expressed in a constitutive manner. The neural stem/progenitor cell marker nestin was also expressed in these CPCs. Immunocytochemical analysis showed that EGFR was hardly detectable in CPCs at 1 DIV but was clearly detected at the plasma membrane and in the cytoplasm at 4 DIV, whereas necdin was predominantly cytoplasmic at 1 and 4 DIV (**Fig. III.1B**). Thus, we used CPCs cultured in the bFGF-supplemented CPC medium for 4 days or more in the following experiments.

We then analyzed autophosphorylation of EGFR in EGF-stimulated CPCs. Autophosphorylation of EGFR (phospho-EGFR), which was detected with a site-specific anti-phosphotyrosine antibody against pY1068, increased markedly in CPCs 5 min after EGF treatment (**Fig. III.2A**). The levels of the total EGFR and phospho-EGFR levels decreased at 120 min. Consistent with the immunoblot results, the phospho-EGFR immunoreactivity increased in the cytoplasm at 5 and 30 min, and both phospho-EGFR and total EGFR levels were reduced at 120 min (**Fig. III.2B**). These results suggest that autophosphorylated EGFR undergoes degradation in primary CPCs.

III-2. Necdin and phosphorylated EGFR colocalize in primary CPCs

We investigated whether EGFR and necdin are colocalized in primary CPCs (**Fig. III.3A**). Immunocytochemistry showed that EGFR was localized at the plasma membrane and in the cytoplasm of CPCs. When CPCs were treated with EGF, EGFR was accumulated in the cytoplasm, and the EGFR immunoreactivity overlapped partially with the necdin immunoreactivity. We also analyzed the colocalization of autophosphorylated EGFR and necdin in CPCs (**Fig. III.3B**). The phospho-EGFR immunoreactivity was hardly detected in unstimulated CPCs but increased appreciably in the cytoplasm of EGF-treated CPCs, where it overlapped partially with that of necdin. Furthermore, three-dimensional analysis of confocal images demonstrated that phospho-EGFR and necdin were colocalized under the plasma membrane (**Fig. III.3C**). We then analyzed the interaction between endogenous necdin and EGFR in CPCs by coimmunoprecipitation assay (**Fig. III.4**). Phospho-EGFR and total EGFR were coprecipitated with necdin in the lysate of wild-type CPCs treated with EGF. Although expression levels of total EGFR were similar between EGF-treated and untreated CPCs, necdin failed to interact with EGFR in wild-type CPCs without EGF treatment. This indicates that necdin binds only to phospho-EGFR. Together, these results suggest that endogenous necdin and phospho-EGFR form a stable complex in EGF-stimulated CPCs.

III-3. Necdin interacts with the TKD of EGFR

To characterize the interaction between necdin and EGFR, we performed the coimmunoprecipitation assay using transfected HEK293A cells. In mouse EGFR cDNA-transfected HEK293A cells, overexpressed EGFR underwent ligand-independent

autophosphorylation (**Fig. III.5A**). To validate the assay system, we tested the interactions of necdin with wild-type EGFR and its kinase dead (K723R) mutant using the adaptor protein Grb2 as a positive control (**Fig. III.5B**). Both necdin and Grb2 bound preferentially to wild-type EGFR, suggesting that necdin binds to EGFR only in its active state.

We then examined the interactions of necdin with EGFR deletion mutants that lack 126 and 240 amino acid residues of the C-tail containing autophosphorylated tyrosine residues (**Fig. III.6A**). Necdin was expressed in transfected HEK293A cells as major 42 kDa and minor 37 kDa proteins (the minor protein is presumably a degraded product of the 42 kDa protein). In this assay, necdin bound to wild-type EGFR (WT) and an EGFR mutant lacking C-terminal 126 residues (WTΔC126) (**Fig. III.6B**). Notably, necdin strongly bound to the deletion mutants WTΔC240 and KRΔC240 lacking the entire C-terminal 240 residues. These results suggest that the C-tail of EGFR interferes with the interaction between necdin and EGFR. Necdin failed to interact with an EGFR mutant (ΔC497) lacking both the C-tail and the tyrosine kinase domain (TKD)(residues 690-946), indicating that necdin binds to the TKD.

To determine the necdin-binding region of the TKD, we constructed Myc-tagged TKD deletion mutants (**Fig. III.7A**). Necdin bound to wild-type TKD and the TKD KR mutant, but not to wild-type TKDΔC91 lacking the C-terminal 91 residues in the C-lobe (**Fig. III.7B**). In contrast, necdin strongly interacted with the C-terminal 91 residues (C91). The necdin-binding region was narrowed down to the C-terminal 30 residues of the TKD (TKD-C30). To test whether necdin directly binds to the TKD-C30 region, we performed *in vitro* pull-down assay using MBP-fused wild-type EGFR TKD (WT), TKD mutants (TKDΔC30 and TKD-C30), and His-tagged necdin (**Fig. III.8A,B**).

Consistent with the results of coimmunoprecipitation, His-tagged necdin bound to wild-type TKD and TKD-C30, but not to TKDΔC30, indicating that necdin binds directly to the C-terminal region (residues 917-946) of the TKD.

III-4. Necdin suppresses the EGFR/ERK signaling

To examine whether endogenous necdin affects the tyrosine kinase activity, we analyzed EGF-induced autophosphorylation of EGFR in necdin-null CPCs (**Fig. III.9A,B**). Immunoblot analysis showed that phospho-EGFR levels were not significantly changed in necdin-null CPCs (**Fig. III.9A,** top panel; **Fig. III.9B**, top graph). We also examined the effects of necdin on the EGFR signaling pathways by analyzing the phosphorylation levels of ERK and Akt. In this analysis, minor and major ERK bands at 44 kDa (ERK1) and 42 kDa (ERK2) were detected. Notably, phospho-ERK levels in necdin-null CPCs increased ~2-fold at 5 min in response to EGF (**Fig. III.9A**, 3rd panel; **Fig. III.9B,** middle graph). In contrast, phospho-Akt levels were not significantly changed in necdin-null CPCs (**Fig. III.9A**, 5th panel, **Fig. III.9B,** bottom graph).

To investigate whether necdin affects the EGFR/RAS/ERK signaling pathway, we examined the interactions of EGFR with the adaptor protein Grb2 and the Grb2-binding RAS activator Sos1 in wild-type and necdin-null CPCs (**Fig. III.10A,B**). The amount of EGFR coprecipitated with Grb2 or Sos1 increased markedly (~2.5-fold) in necdin-null CPCs treated with EGF (**Fig. III.10A**, top and 3rd panels, **Fig. III.10B**). Grb2 failed to interact with necdin as analyzed by coimmunoprecipitation using transfected HEK293A (**Fig. III.11**). These results suggest that necdin suppresses the interaction between EGFR and Grb2 to downregulate the RAS/ERK signaling in CPCs.

III-5. Necdin suppresses proliferation of CPCs

Because the EGFR/ERK pathway is involved in the control of cellular proliferation, we next examined whether necdin affects the proliferation rate of primary CPCs (**Fig. III.12A,B**). When CPCs were treated with EGF for 48 h, the total cell number of CPCs increased significantly (1.37 times the wild-type control level) in necdin-null CPCs, whereas there was no significant difference in the absence of EGF. We also used EdU incorporation assay to determine the proliferation rate of CPCs prepared from wild-type and necdin-null mice (**Fig. III.13A-C**). The population of EdU^+ S-phase cells in necdin-null CPCs increased significantly (1.35 times the wild-type control level). These results suggest that endogenous necdin suppresses EGF-stimulated proliferation of primary CPCs through inhibition of the EGFR/ERK pathway. To elucidate the downregulation of RAS/MEK/ERK signaling pathway, we determined the mRNA levels of immediate early gene in CPCs prepared from wild-type and necdin-null mice after EGF treatment (**Fig. III.14**). The cFOS mRNA level increased significantly in the necdin-null CPCs, whereas no significant differences in the cJUN, EGR1, and EGR2 mRNA levels were noted between wild-type and necdin-null mice. Interestingly, the mRNA level of IEX1, an immediate early gene related to astrocyte differentiation (You et al., 2007), increased significantly in CPCs from necdin-deficient mice.

III-6. Necdin suppresses astrocyte differentiation of CPCs

CPCs differentiate into astrocytes in response to the interleukin-6 (IL-6) family of cytokines such as CNTF and LIF (Bonni et al., 1997; Johe et al., 1996; Nakashima et al., 1999). EGFR regulates the competence of CPCs to interpret LIF as an

astrocyte-inducing signal (Viti et al., 2003). To investigate whether necdin affects astrocyte differentiation of CPCs by suppressing EGFR signaling, we used cardiotrophin-1 (CT-1), one of the IL-6 family cytokines (Barnabe-Heider et al., 2005; Ochiai et al., 2001), to induce astrocyte differentiation of CPCs (**Fig. III.15A-C**). The number of $GFAP^+$ astrocytes differentiated from necdin-null CPCs increased by 39% in the presence of EGF and CT-1, whereas the $GFAP^+$ cell population was not significantly changed in necdin-null CPCs in the absence of EGF. These results indicate that endogenous necdin suppresses EGF-promoted glial differentiation via inhibition of the EGFR/ERK signaling.

In this analysis, we found that the GFAP immunoreactivity increased appreciably in each GFAP-expressing cell differentiated from necdin-null CPCs (**Fig. III.15B**). Thus, we analyzed the expression levels of the GFAP protein by immunoblotting (**Fig. III.15D**). EGF markedly increased expression levels of the GFAP protein in necdin-null CPCs treated with CT-1, indicating that the GFAP protein level correlates well with the extent of astrocyte differentiation.

We also examined neuronal differentiation of EGF-treated CPCs by withdrawing both bFGF and EGF (**Fig. III.16A-C**). EGF markedly reduced the population of βIII-$tubulin^+$ neurons, suggesting that EGF prevents neuronal differentiation of CPCs. However, there was no significant difference in the number of differentiated βIII-$tubulin^+$ neurons between wild-type and necdin-null CPCs. These observations suggest that necdin specifically suppresses EGF-promoted astrocyte differentiation of CPCs.

To investigate whether necdin-null mice express high GFAP levels in the cortex *in vivo* during the neonatal period, we analyzed cortical GFAP levels at postnatal day 4 by

immunoblotting. We found no significant difference in the GFAP level between wild-type and necdin-null mice (**Fig. III.17A,B**). Intriguingly, EGF mRNA levels in necdin-null cortex *in vivo* were reduced by 54% at E18.5, a late stage of cortical development when astrocyte differentiation occurs (**Fig. III.17C**). Expression of EGF mRNA in primary CPCs was also reduced by 50% (**Fig. III.17D**). These results suggest that necdin-null CPCs express low levels of EGF mRNA to prevent astrocyte hyperproliferation due to enhanced EGFR signaling via a negative feedback regulation.

III-7. Inhibition of EGFR/ERK signaling blocks astrocyte differentiation

To determine whether EGF-promoted astrocyte differentiation is mediated via the EGFR signaling pathways in CPCs, we used the EGFR tyrosine kinase inhibitor (gefitinib), MEK1/2 inhibitor (U0126), and PI3K inhibitor (LY294002). We first examined the effects of these inhibitors on EGF-induced phosphorylation levels of EGFR, ERK and Akt by immunoblot analysis (**Fig. III.18A**). Autophosphorylation of EGFR was detected 5 min after EGF stimulation in CPCs treated with the MEK inhibitor and the PI3K inhibitor but not in those treated with the EGFR tyrosine kinase inhibitor. As expected, phosphorylation of ERK and Akt was hardly detected in EGF-stimulated CPCs treated with the inhibitors of MEK and PI3K, respectively.

We then analyzed the effects of these kinase inhibitors on astrocyte differentiation by immunoblot assay. CPCs were treated with EGF in the presence or absence of these inhibitors for 6 h and then with CT-1 for 48 h (**Fig. III.18B**). The GFAP levels in EGF-stimulated CPCs increased appreciably when incubated in the absence of the inhibitors or in the presence of the PI3K inhibitor (**Fig. III.18C**). These observations indicate that EGF-promoted astrocyte differentiation is mediated by the EGFR/ERK

signaling pathway in CPCs.

To test whether the EGFR/RAS/MEK/ERK pathway mediates EGF-promoted enhancement of the GFAP levels in necdin-null CPCs, we treated CPCs with EGF and these kinase inhibitors (**Fig. III.19A,B**). The EGF-dependent increase in the GFAP levels was significantly enhanced (1.54 times the wild-type control level) in necdin-null CPCs, and this enhancement was completely blocked by EGFR tyrosine kinase inhibitor (gefitinib) or MEK1/2 inhibitor (U0126), but not by PI3K inhibitor (LY294002). These results suggest that necdin suppresses astrocyte differentiation through attenuation of the EGFR/RAS/MEK/ERK signal transduction.

III-8. Necdin suppresses EGFR-promoted astrocyte differentiation

Sustained activation of the EGFR/RAS/ERK pathway is involved in astrocyte proliferation and pathogenesis of gliomas (Nicholas et al., 2006; Zhu and Parada, 2002). Thus, we investigated whether astrocyte differentiation of primary CPCs is promoted by overexpression of EGFR and an EGFR mutant (EGFRΔNT) lacking the N-terminal ligand-binding domain (L1), which is equivalent to human glioblastoma-associated EGFR variant III (EGFRvIII) (**Fig. III.20A**). CPCs were transiently transfected with cDNAs encoding wild-type EGFR, kinase-dead K723R mutant, and EGFRΔNT by electroporation. Autophosphorylation of wild-type EGFR and EGFRΔNT mutant, but not that of the KR mutant, was detected 12 h after transfection by immunoblot analysis of phospho-EGFR (**Fig. III.20B**).

We analyzed whether forced expression of EGFR and EGFR mutants enhances astrocyte differentiation. Transiently transfected CPCs were incubated for 24 h and then treated with CT-1 for 48 h (**Fig. III.21A**). Immunocytochemistry showed that

overexpression of wild-type EGFR or EGFRΔNT increased the GFAP immunoreactivity in transfected td-Tomato$^+$ CPCs (**Fig. III.21B**). These cells exhibited morphological characteristics of differentiated astrocytes such as extended processes and larger cell bodies. Consistent with these morphological changes, GFAP expression levels increased markedly in CPCs transfected with wild-type EGFR or EGFRΔNT as analyzed by immunoblotting (**Fig. III.21C)**.

We then examined whether necdin prevents EGFR- or EGFRΔNT-promoted astrocyte differentiation of CPCs (**Fig. III.22A,B**). We found that a necdin mutant lacking residues 144-184 located in the MAGE homology domain (necdinΔEB) (Taniura et al., 2005) failed to interact with EGFR (**Fig. III.23A,B**). Thus, we used this EGFR binding-defective mutant as a negative control. Necdin strongly decreased the GFAP level to near basal level of td-Tomato$^+$ control in EGFR-overexpressing CPCs. Similarly, necdin reduced the GFAP level in EGFRΔNT-overexpressing CPCs. In contrast, necdinΔEB had no antagonizing effects. In this analysis, neither necdin nor necdinΔEB affected the basal GFAP level in transfected CPCs.

We analyzed whether human MAGEA1, a MAGE family member expressed in many cancers, affects EGFR-mediated astrocyte differentiation induced by EGFR overexpression. MAGEA1 bound to both EGFR and kinase-dead mutant (**Fig. III.24A,B**). To determine the MAGEA1-binding region of the TKD, we constructed Myc-tagged TKD deletion mutants (**Fig. III.25A**). MAGE-A1 bound to wild-type TKD and TKDΔC91 lacking the C-terminal 91 residues in the C-lobe but not to TKDΔPL, TKDΔCH, and TKDΔAL which are important for TKD activation (**Fig. III.25B**). In contrast to necdin, MAGEA1 enhanced EGFR-induced GFAP expression, and

coexpression of necdin strongly antagonized the effect of MAGEA1 (**Fig. III.26A,B**). These results suggest that necdin and MAGEA1 exert opposite effects on the EGFR signaling.

We also examined the GFAP expression levels in wild-type and necdin-null CPCs overexpressing EGFR (**Fig. III.27A,B**). The GFAP levels increased by 57% in necdin-null CPCs overexpressing EGFR. The increase in the GFAP level was completely suppressed by coexpression of necdin, but not of necdinΔEB. These results suggest that endogenous necdin in CPCs acts as an intrinsic suppressor of astrocyte differentiation induced by EGFR overexpression.

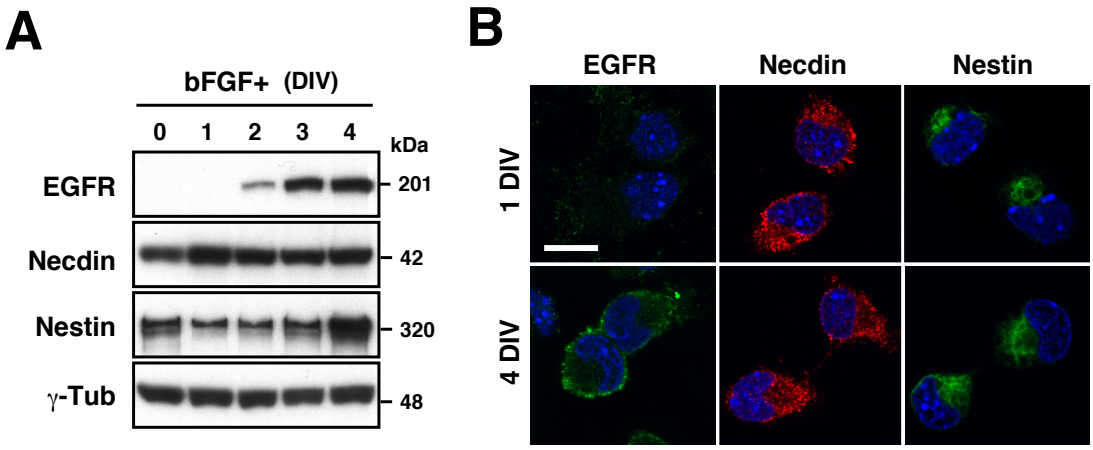

Figure III.1 EGFR and necdin are coexpressed in primary CPCs.
(**A**) CPCs were prepared from the neocortex at E14.5 and cultured in the presence of bFGF (bFGF+) for the indicated durations. Expression of EGFR, necdin, nestin, and γ-tubulin (γ-Tub) was analyzed by immunoblotting. (**B**) CPCs were immunostained for EGFR (green), necdin (red), and nestin (green) and observed by confocal microscopy. Nuclear DNA was counterstained with Hoechst33342 (blue) and merged with confocal images. Scale bar; 10 μm (in **B**)

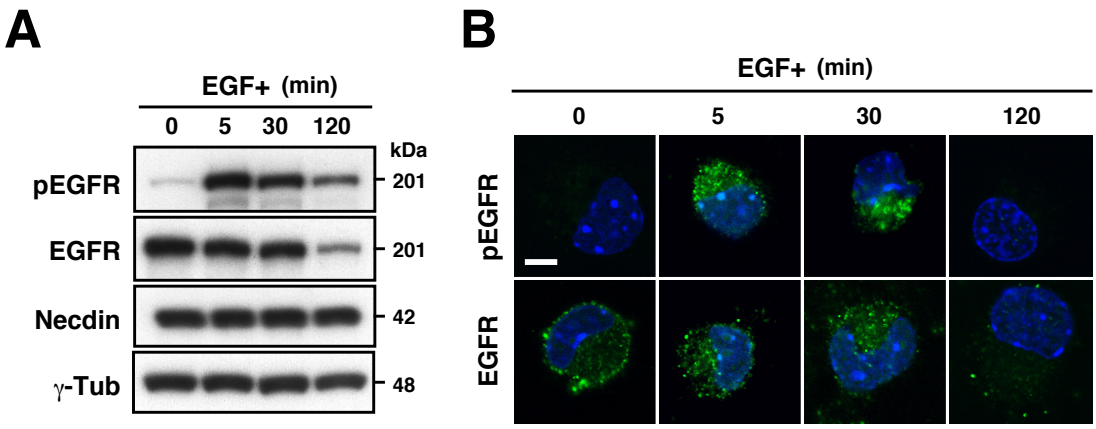

Figure III.2 Autophosphorylation occurs by addition of EGF in primary CPCs.

(**A**) CPCs were treated with EGF for the indicated durations. Expression of phospho-EGFR (pEGFR) and total EGFR (EGFR) was analyzed by immunoblotting or (**B**) immunocytochemistry. Confocal images (green) and nuclear DNA stain (blue) are merged. Scale bar; 5 μm (in **B**).

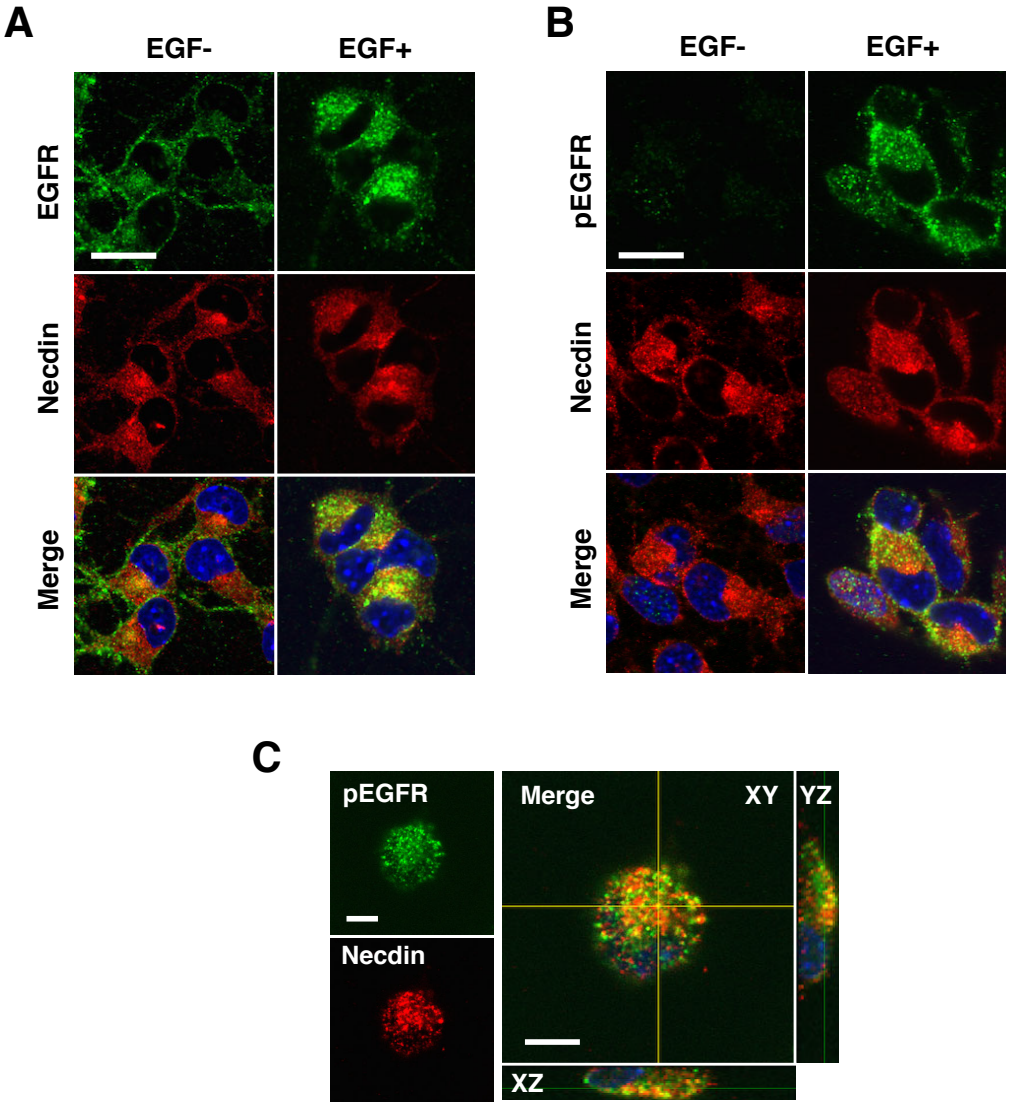

Figure III.3 Autophosphorylated EGFR and necdin are colocalized in primary CPCs.

(**A, B**) Immunocytochemistry. CPCs at 4 DIV were treated with (EGF+) or without (EGF-) EGF for 5 min. EGFR (green)(**A**) or phospho-EGFR (pEGFR)(green)(**B**) and necdin (red) were immunostained and observed by confocal microscopy. Immunostained images and nuclear DNA stain (blue) are merged (Merge) for colocalization (yellow). (**C**) Three-dimensional analysis. CPCs were double immunostained for pEGFR (green) and necdin (red), and observed by confocal microscopy. Multiple z-stack images in XY, XZ and YZ axes are shown. Scale bars; 10 μm (in **A, B**), 5 μm (in ***C***).

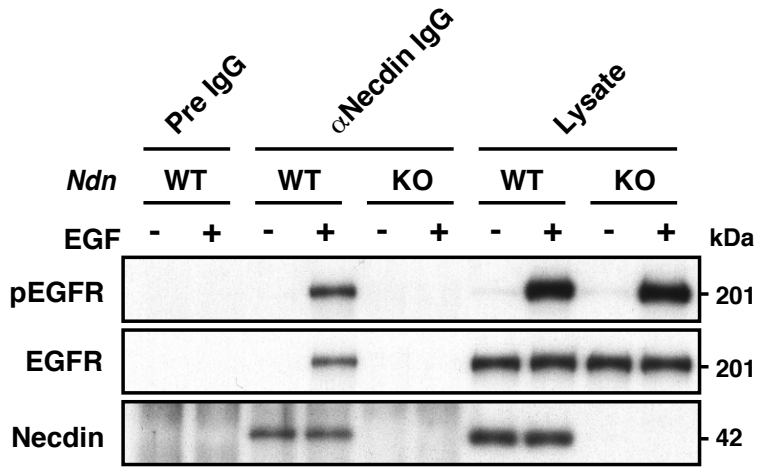

Figure III.4 Endogenous necdin interacts with phospho-EGFR in CPCs. Coimmunoprecipitation assay. CPCs were prepared from wild-type (WT) and necdin-null (KO) mice and treated at 4 DIV with EGF (EGF+) or without (EGF-) EGF for 5 min. Cell lysates were immunoprecipitated with anti-necdin IgG (αNecdin IgG) or preimmune IgG (Pre IgG). pEGFR, EGFR, and necdin were analyzed by immunoblotting. Lysate, CPC lysate (10 μg).

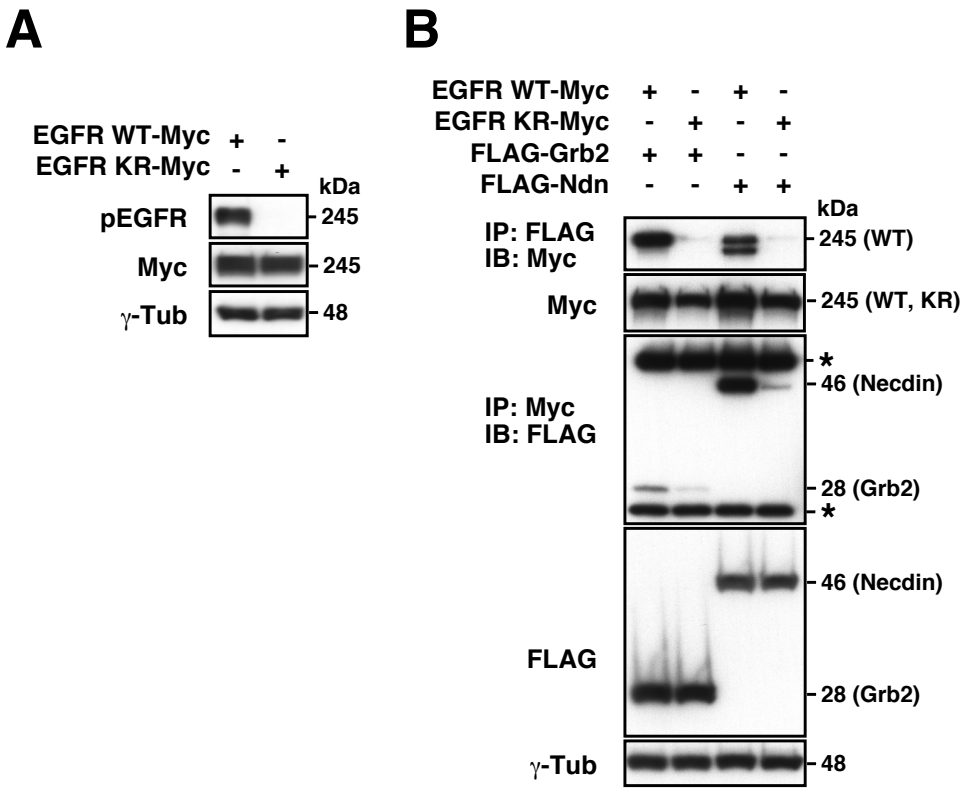

Figure III.5 Autophosphorylated EGFR binds to necdin and Grb2 in HEK293A cells.

(**A**) HEK293A cells were transfected with cDNAs for Myc-tagged EGFR and its kinase dead K723R mutant. Autophosphorylation was detected with antibody against phospho-EGFR (pEGFR). (**B**) HEK293A cells were transfected with cDNAs for Myc-tagged wild-type EGFR (WT), Myc-tagged K723R mutant (KR), FLAG-tagged Grb2 (FLAG-Grb2, positive control) and FLAG-tagged necdin (FLAG-Ndn). Cell lysates were immunoprecipitated (IP) with antibodies to FLAG and Myc, and immunoblotted (IB) for Myc, FLAG, and γ-tubulin (γ-Tub). Asterisks indicate non-specific IgG bands.

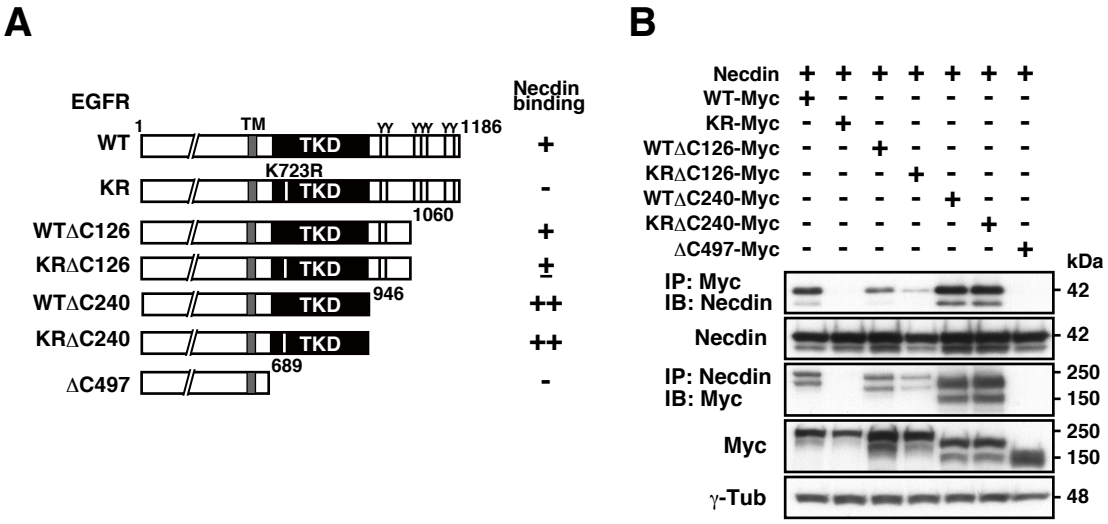

Figure III.6 Necdin interacts with the tyrosine kinase domain of EGFR.
(**A**) Diagrams of EGFR and its C-terminal-truncated mutants. WT, wild-type; KR, K723R mutant; ΔC126, C-terminal 126 residue deletion; ΔC240, C-terminal 240 residue deletion; ΔC497, C-terminal 497 residue deletion; TM, transmembrane domain; TKD, tyrosine kinase domain; Y, autophosphorylated tyrosine residues.
(**B**) HEK293A cells were co-transfected with cDNAs for Myc-tagged EGFR (WT, KR) and necdin. Cell lysates were immunoprecipitated (IP) with antibodies to Myc and necdin, and immunoblotted (IB) for necdin, Myc, and γ-tubulin (γ-Tub). Results are shown in ***A***.

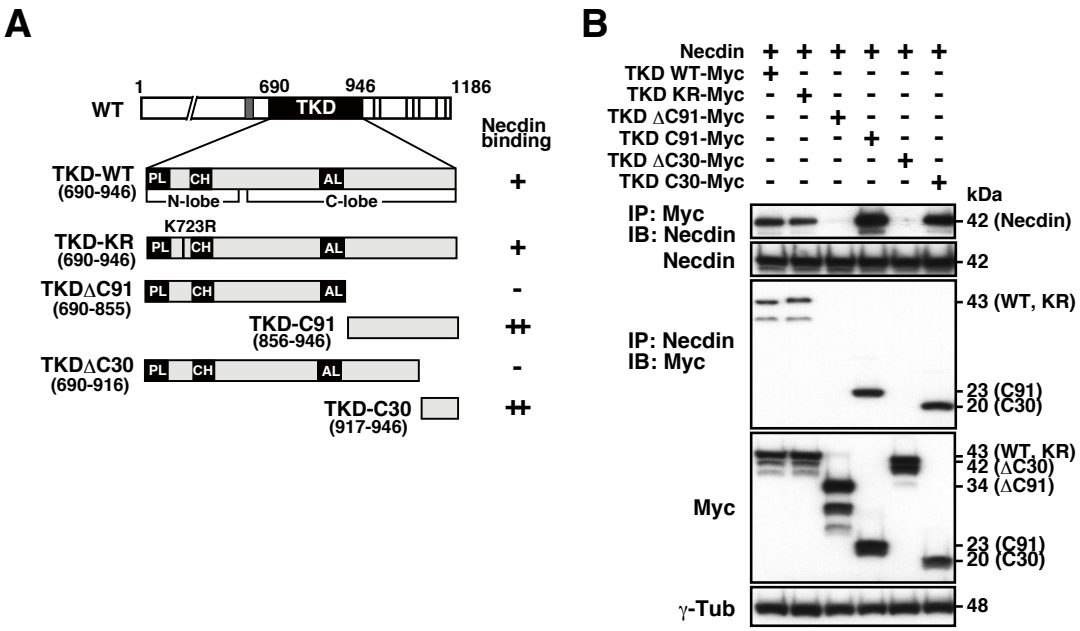

Figure III.7 Necdin strongly interacts with the C-terminal 30 residues of EGFR tyrosine kinase domain.

(**A**) Diagrams of TKD deletion mutants. TKD-WT, wild-type TKD; TKD-KR, K723R mutant TKD; TKDΔC91, C-terminal 91 residue deletion; TKDΔC30, C-terminal 30 residue deletion; TKD-C91, C-terminal 91 residues; TKD-C30, C-terminal 30 residues; PL, phosphate-binding loop; CH, C-helix; AL, activation loop. (**B**) Coimmunoprecipitation assay for TKD-deletion mutants. HEK293A cells were co-transfected with cDNAs for Myc-tagged TKD mutants and necdin. Cell lysates were immunoprecipitated (IP) with antibodies to Myc and necdin and immunoblotted (IB) for necdin and Myc. Results are shown in **A**.

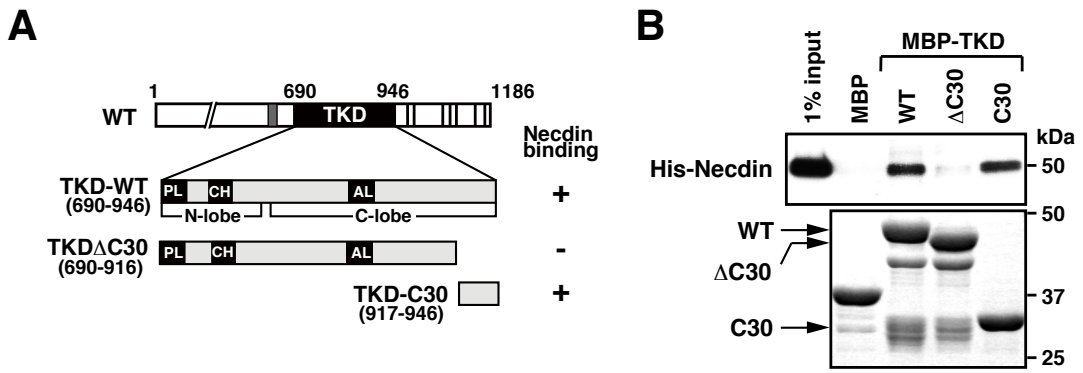

Figure III.8 Necdin directly binds to the C-terminal 30 residues of EGFR tyrosine kinase domain.

(**A**) Diagrams of TKD deletion mutants. TKD-WT, wild-type TKD; TKDΔC30, C-terminal 30 residue deletion; TKD-C30, C-terminal 30 residues; PL, phosphate-binding loop; CH, C-helix; AL, activation loop. (**B**) *In vitro* binding assay. Purified maltose-binding protein (MBP)-fused EGFR deletion mutants immobilized on amylose resin were incubated with His-tagged necdin (His-Necdin). Bound His-necdin was detected by immunoblotting with anti-necdin antibody (upper panel). MBP-EGFR TKD mutants were separated by 7.5% SDS-PAGE and stained with Coomassie Brilliant Blue (lower panel). Results are shown in **A**.

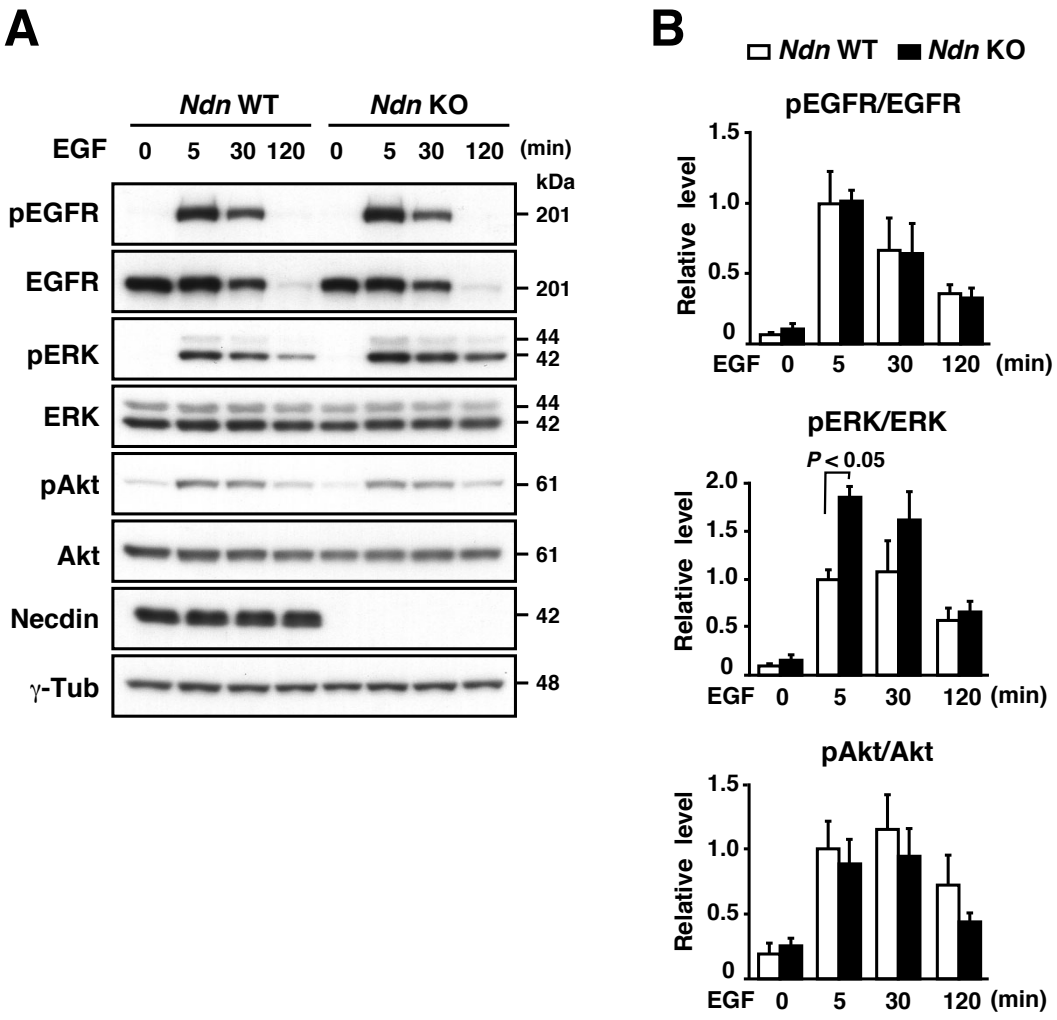

Figure III.9 Necdin suppresses the EGFR/ERK signaling pathway in CPCs.

(**A, B**) EGF-induced phosphorylation of EGFR, ERK, and Akt. CPCs prepared from wild-type (*Ndn* WT) and necdin-null (*Ndn* KO) mice at E14.5 were cultured for 4 days and treated with EGF (10 ng/ml) for the indicated durations. CPC lysates were immunoblotted for phospho-EGFR (pEGFR), EGFR, phospho-ERK (pERK), ERK, phospho-Akt (pAkt), Akt, necdin, and γ-tubulin. pEGFR, pERK and pAkt levels were quantified by densitometry and normalized to those of EGFR, ERK and Akt, respectively, and then to γ-tubulin (**B**). Each value represents the mean ± SEM, $n = 3$ (pEGFR), $n = 4$ (pERK, pAkt). *P*-values were calculated using one-way ANOVA followed by Tukey-Kramer *post hoc* test.

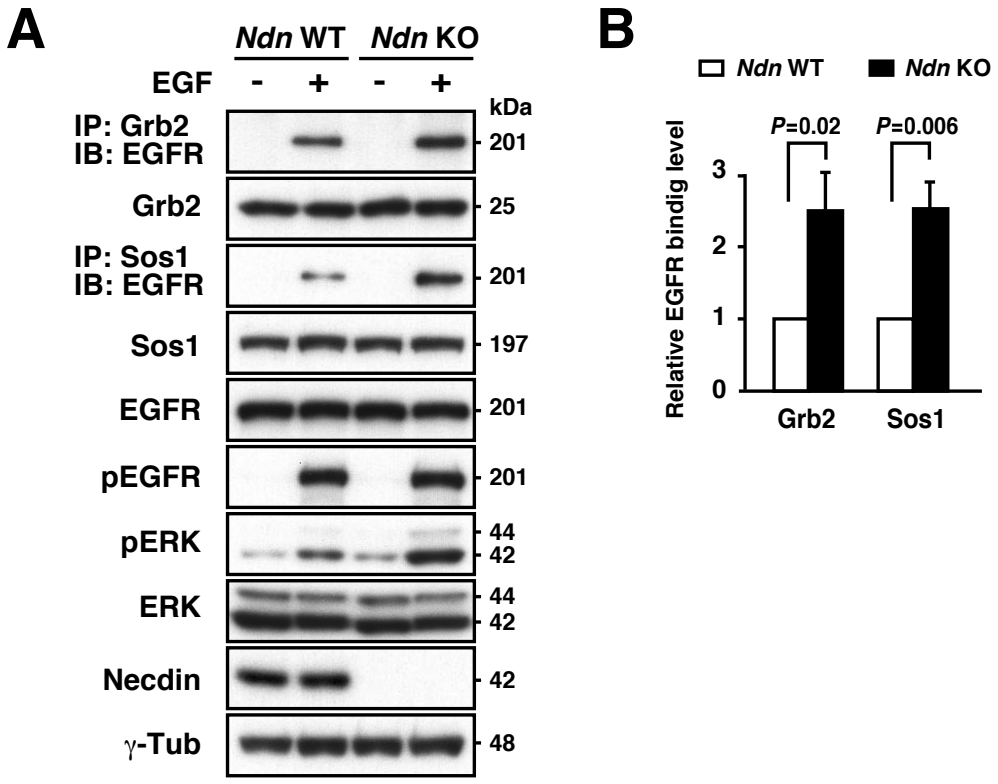

Figure III.10 Necdin inhibits the interaction between EGFR and Grb2/Sos1 in CPCs.

(**A, B**) Interactions of EGFR with Grb2 and Sos1 in EGF-stimulated CPCs. CPCs at 4 DIV were treated with (EGF+) or without (EGF-) EGF for 5 min. CPC lysates were immunoprecipitated (IP) with antibodies to Grb2 and Sos1 and immunoblotted (IB) for EGFR, Grb2, Sos1, pEGFR, pERK, ERK, necdin, and γ-tubulin (**A**). Signal densities of EGFR coprecipitated with Grb2 and Sos1 were normalized to those of Grb2 and Sos1, respectively, and then to γ-tubulin (**B**). Each value represents the mean ± SEM (Grb2, $n = 6$; Sos1, $n = 4$). *P*-values were calculated using Student's *t*-test.

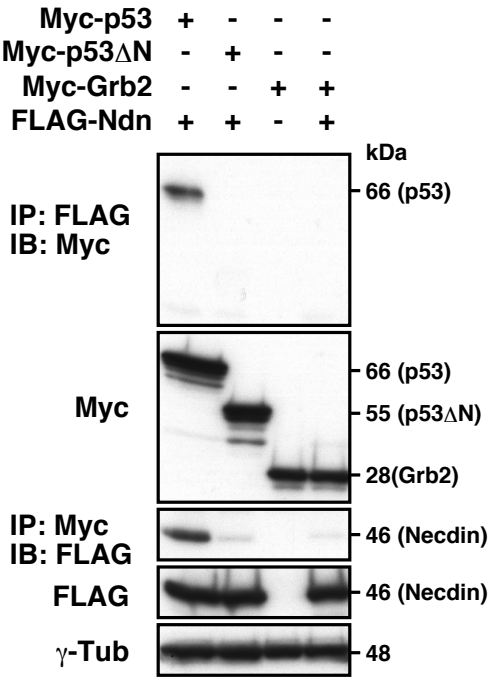

Figure III.11 Necdin fails to interact with Grb2.
Interaction between necdin and Grb2. HEK293A cells were transfected with cDNAs for Myc-tagged p53 (Myc-p53, positive control) and its N-terminal truncated mutant p53ΔN (Myc- p53ΔN, negative control)(Taniura et al., 1999) and Myc-tagged Grb2 (Myc-Grb2) and Myc-tagged necdin (Myc-Ndn). Cell lysates were immunoprecipitated (IP) with antibodies to FLAG and Myc, and immunoblotted (IB) for Myc, FLAG, and γ-tubulin (γ-Tub).

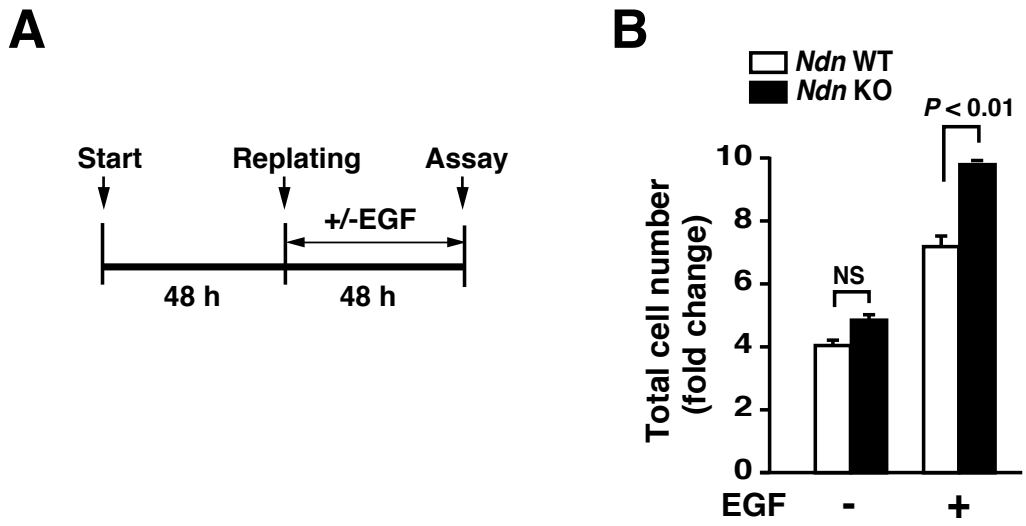

Figure III.12 Necdin suppresses EGF-promoted proliferation of CPCs.
(**A, B**) Total CPC count. CPCs prepared from wild-type (*Ndn* WT) and necdin-null (*Ndn* KO) E14.5 mice were cultured for 48 h, replated at 2 x 10^5 cells per 35-mm dish, and cultured in the presence (EGF+) or absence (EGF-) of EGF for another 48 h (**A**). Cells were harvested for manual cell counting ($n = 4$) and presented as fold change (**B**). *P*-values were calculated using one-way ANOVA followed by Tukey-Kramer *post hoc* test. NS, not significant at $P \geq 0.05$.

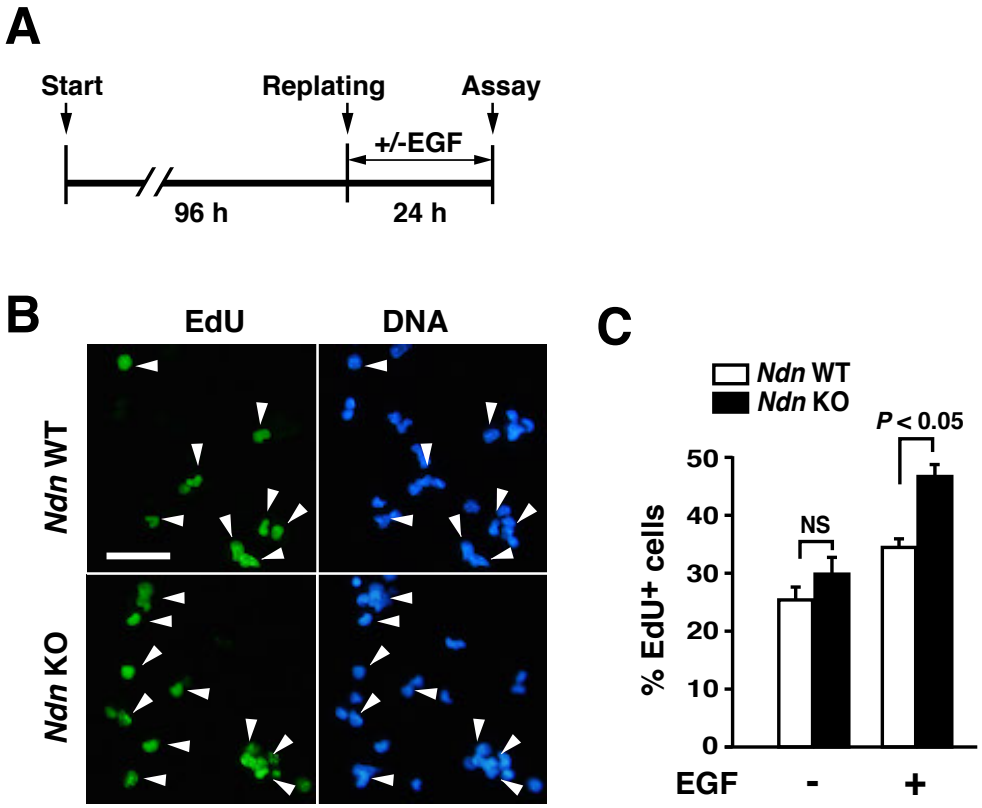

Figure III.13 The population of EdU$^+$ S-phase cells in necdin-null CPCs increased significantly.

(**A-C**) EdU incorporation assay. CPCs were cultured for 96 h, replated onto poly-L-ornithine-precoated 24-well plates, cultured in the presence (EGF+) or absence (EGF-) of EGF for 24 h, and fixed for fluorescence microscopy (**B**). EdU was added to the medium 4 h before fixation, and EdU incorporated into nuclear DNA was chemically stained (green, arrowheads). EdU$^+$ cells were counted (each >190 DNA-stained cells examined, n = 3), and the EdU$^+$ population is presented as percentage (**C**). *P*-values were calculated using one-way ANOVA followed by Tukey-Kramer *post hoc* test. NS, not significant at $P \geq 0.05$.

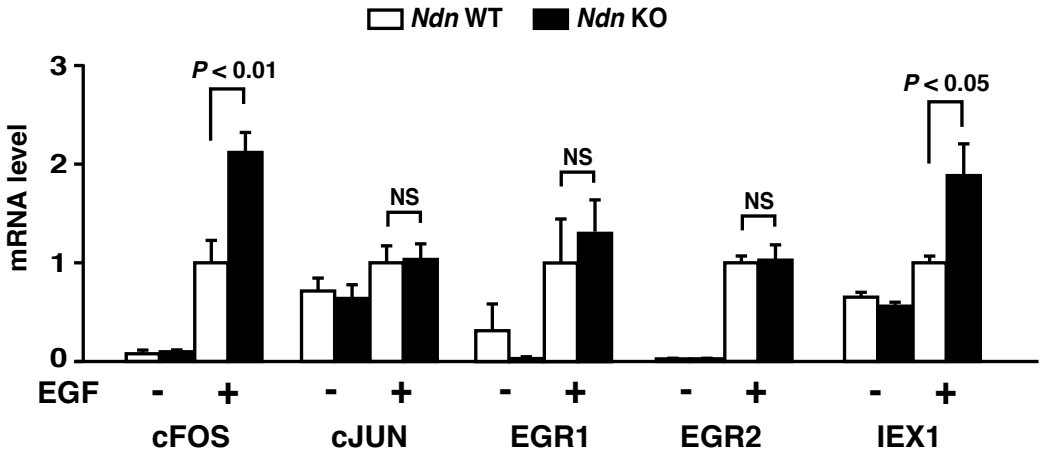

Figure III.14 Expression of immediate early genes in wild-type and necdin-deficient CPCs.

Expression levels of the immediate early genes cFOS, cJUN, EGR1, EGR2, and IEX1 in EGF-treated CPCs prepared from wild-type (*Ndn* WT) and necdin-null (*Ndn* KO) mice were analyzed by qRT-PCR. *P*-values were calculated using one-way ANOVA followed by Tukey-Kramer *post hoc* test. $n = 4$. NS, not significant at $P \geq 0.05$.

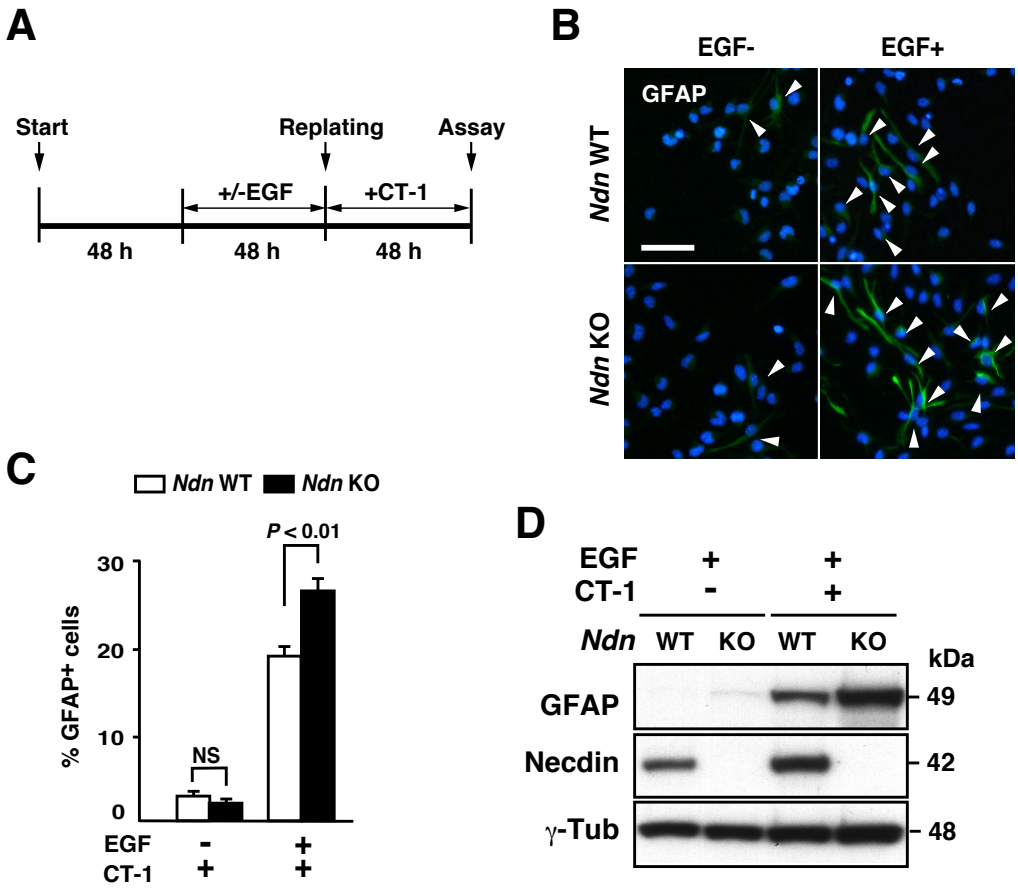

Figure III.15 Necdin suppresses EGF-promoted astrocyte differentiation of CPCs.

(**A**-**C**) Astrocyte differentiation assay. CPCs prepared from wild-type (*Ndn* WT) and necdin-null (*Ndn* KO) mice at E14.5 were cultured for 48 h, treated with (EGF+) or without (EGF-) EGF for 48 h, and then with CT-1 for 48 h (**A**). CPCs were immunostained for GFAP (green)(**B**), and $GFAP^+$ cells were counted (each >170 cells examined, $n = 3$)(**C**). (**D**) Expression of GFAP in CPCs treated with EGF in the presence (CT-1+) or absence (CT-1-) of CT-1 was analyzed by immunoblotting. Immunostained images are merged with nuclear DNA stain (**B**). Scale bar, 50 μm (in **B**). Each value represents the mean ± SEM (in **C**). *P*-values were calculated using one-way ANOVA followed by Tukey-Kramer *post hoc* test. NS, not significant at $P \geq 0.05$.

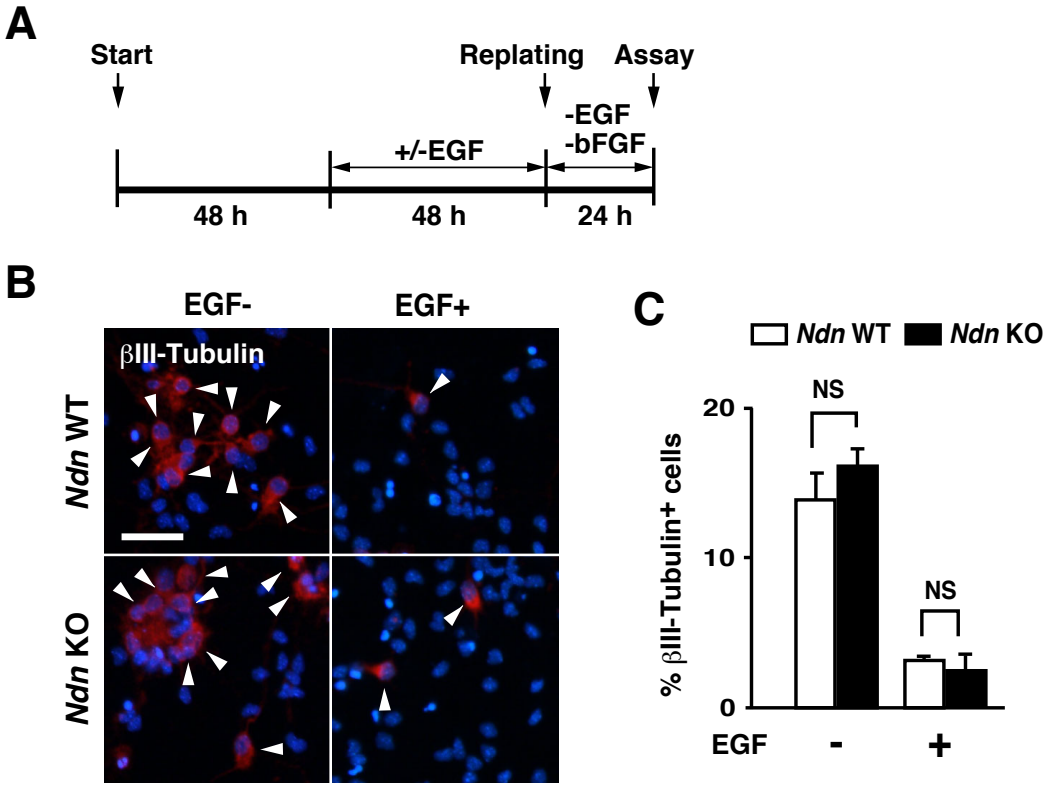

Figure III.16 Necdin fails to affect neuronal differentiation.
(**A**-**C**) Neuronal differentiation assay. CPCs were cultured for 48 h, treated with (EGF+) or without (EGF-) EGF for 48 h and incubated in the medium deprived of EGF and bFGF for 24 h (**A**). CPCs were immunostained for βIII-tubulin (red)(**B**), and βIII-tubulin$^+$ cells were counted (each >300 cells examined, $n = 3$)(**C**). Immunostained images are merged with nuclear DNA stain (**B**). Scale bar, 50 μm (in **B**). Each value represents the mean ± SEM (in **C**). *P*-values were calculated using one-way ANOVA followed by Tukey-Kramer *post hoc* test. NS, not significant at $P \geq 0.05$.

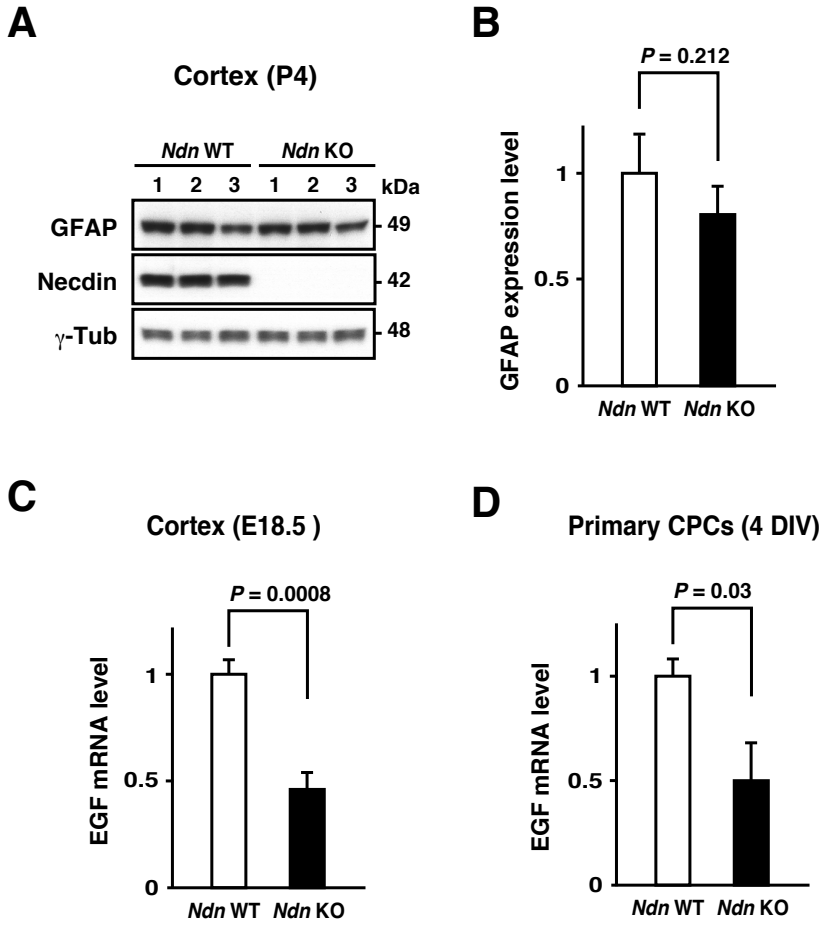

Figure III.17 Expression of the GFAP protein and EGF mRNA in necdin-null neocortex *in vivo.*

(**A**, **B**) GFAP protein levels in the neocortex *in vivo*. Neocortical tissues were prepared from wild-type (*Ndn* WT) and necdin-null (*Ndn* KO) mice at postnatal day 4 (P4). GFAP protein levels were analyzed by Western blotting and quantified by densitometry (**B**). Each value represents the mean ± SEM, $n = 3$. *P*-values were calculated using Student's *t*-test. (**C, D**) EGF mRNA levels. Expression levels of EGF in the neocortex at E18.5 (**C**) and primary CPCs at 4 DIV (**D**) were analyzed by quantitative RT-PCR (qRT-PCR). Each value represents the mean ± SEM (neocortex; $n = 5$, CPCs; $n = 3$). *P*-values were calculated using Student's *t*-test.

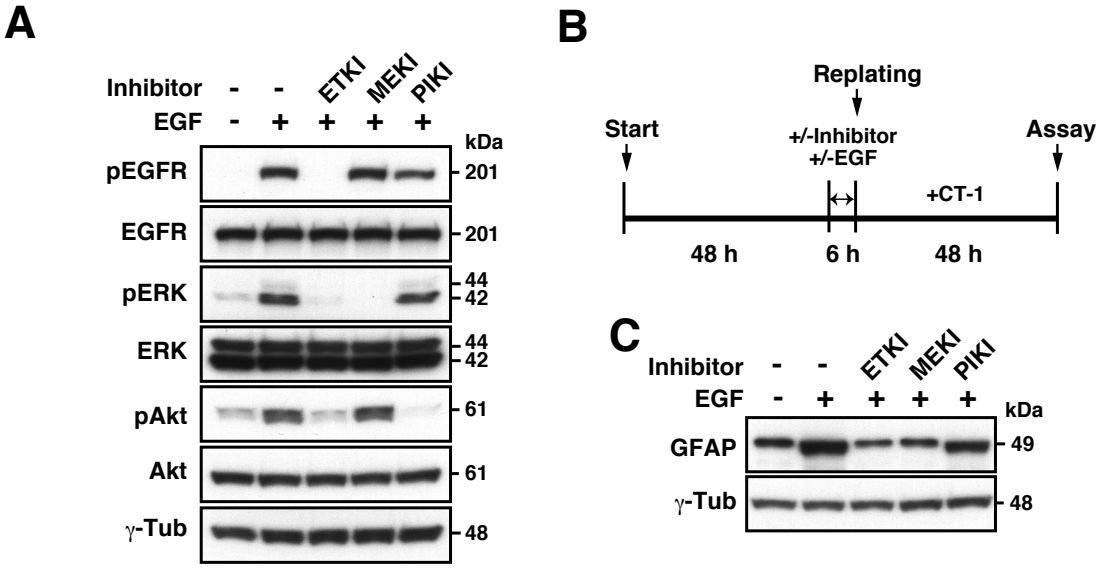

Figure III.18 EGF-promoted astrocyte differentiation is mediated by the EGFR/ERK signaling pathway in CPCs.

(**A**) Effects of kinase inhibitors on EGFR signaling pathways. CPCs were incubated for 48 h and treated with EGF for 5 min. EGFR tyrosine kinase inhibitor (ETKI, gefitinib; 5 μM), MEK inhibitor (MEKI, U0126; 20 μM) and PI3K inhibitor (PIKI, LY294002; 20 μM) were added to the medium 30 min before EGF treatment. Phospho-EGFR (pEGFR), phospho-ERK (pERK), and phospho-Akt (pAkt) levels in CPCs were analyzed by immunoblotting. (**B**, **C**) GFAP expression in CT-1-treated CPCs. CPCs were cultured for 48 h, treated with EGF (EGF+) or without (EGF-) EGF and kinase inhibitors for 6 h, and incubated with CT-1 for 48 h (**B**). GFAP expression in CPCs was analyzed by immunoblotting (**C**).

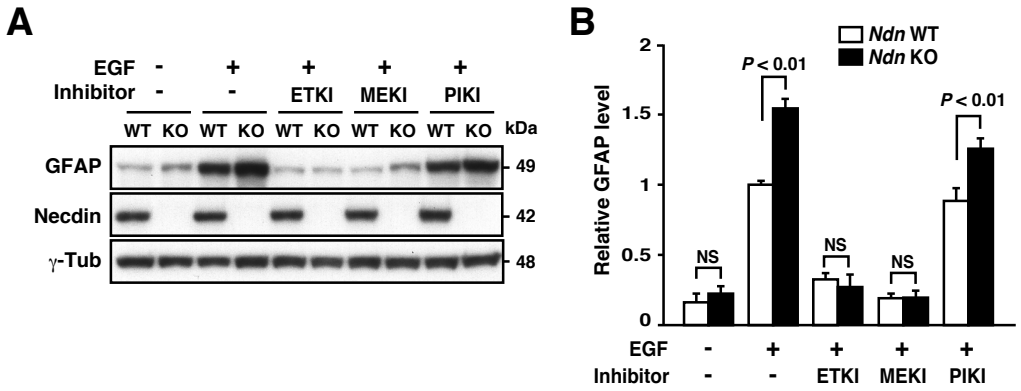

Figure III.19 Necdin suppresses EGF-promoted GFAP expression in CPCs. (**A**, **B**) Effects of kinase inhibitors on GFAP levels in necdin-null CPCs. CPCs prepared from wild-type (*Ndn* WT) and necdin-null (*Ndn* KO) E14.5 mice were treated with EGF and kinase inhibitors as in **Fig III.18B.** Expression of GFAP, necdin, and γ-tubulin (γ-Tub) was analyzed by immunoblotting (**A**) and quantified by densitometry (**B**). GFAP levels were normalized to γ-tubulin levels. Each value represents the mean ± SEM, $n = 4$. *P*-values were calculated using one-way ANOVA followed by Tukey-Kramer *post hoc* test. NS, not significant at $P \geq 0.05$.

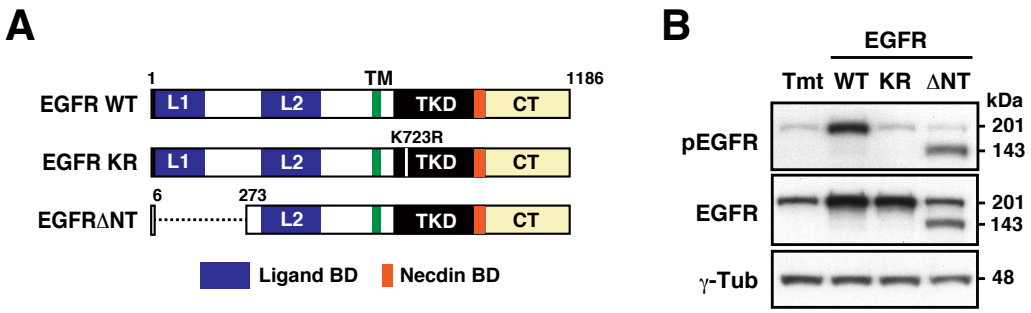

Figure III.20 Overexpression of EGFR induce autophosphorylation without EGF stimulation.

(**A**) Diagrams of EGFR and its mutants. WT, wild-type EGFR; KR, EGFR K723R mutant; ΔNT, EGFR N-terminal (residues 6-273) deletion mutant; L1/2, ligand-binding domain 1/2 (Ligand BD) ; TM, transmembrane domain; Necdin BD, necdin-binding domain; TKD, tyrosine kinase domain; CT, C-terminal domain. (**B**) Autophosphorylation of EGFR and ΔNT mutant. CPCs were transiently transfected with wild-type EGFR, KR mutant and ΔNT mutant by electroporation, and expression of phospho-EGFR (pEGFR) and EGFR in transfected CPCs was analyzed 12 h after transfection by immunoblotting. Tmt, td-Tomato vector control.

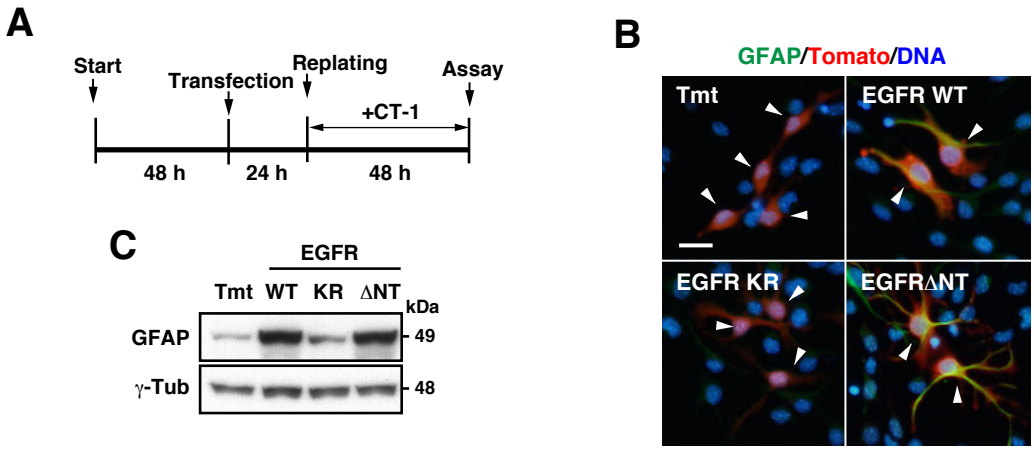

Figure III.21 Overexpression of EGFR enhances astrocyte differentiation. (**A**-**C**) GFAP expression in EGFR-overexpressing CPCs. CPCs were transiently transfected with cDNAs for wild-type EGFR and its mutants, cultured for 24 h, and treated with CT-1 for 48 h (**A**). GFAP expression in transfected CPCs was analyzed by triple staining of GFAP (green), td-Tomato (red), and nuclear DNA (blue)(**D**) and immunoblotting (**B**). Triple-stained images are merged for GFAP expression in td-Tomato^{+} cells (yellow in **C**). Arrowheads point to td-Tomato^{+} CPCs. Scale bar, 20 μm.

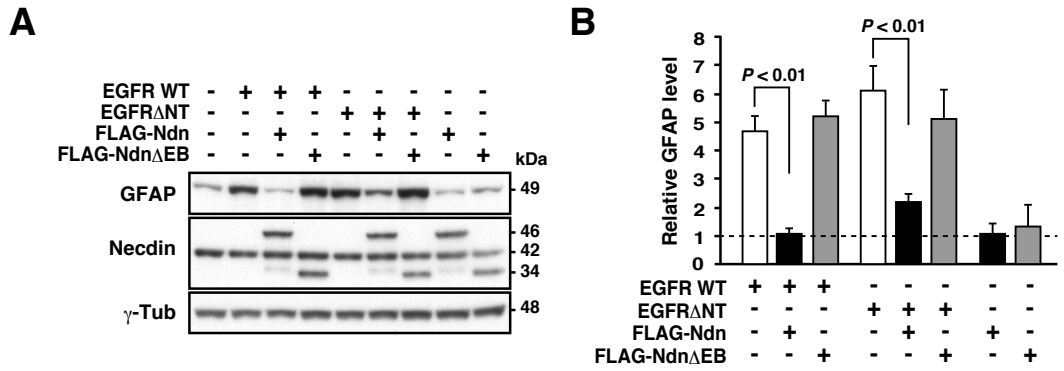

Figure III.22 Necdin suppresses EGFR- and EGFRΔNT-promoted astrocyte differentiation of CPCs

(**A**, **B**) Effect of necdin on EGFR-induced GFAP expression. CPCs were transiently transfected with combinations of cDNAs for wild-type EGFR, EGFRΔNT, FLAG-necdin (Ndn) and NdnΔEB (EGFR binding-defective necdin mutant). GFAP expression in transfected CPCs was analyzed immunoblotting (**A**). Necdin-immunoreactive bands at 46, 42, 34 kDa are of FLAG-necdin, endogenous necdin, and necdinΔEB, respectively. GFAP expression was quantified by densitometry (**B**). The broken line indicates the basal GFAP expression in CPCs expressing td-Tomato alone (=1). Each value represents the mean ± SEM, $n = 4$. *P*-values were calculated using one-way ANOVA followed by Tukey-Kramer *post hoc* test. NS, not significant at $P \geq 0.05$.

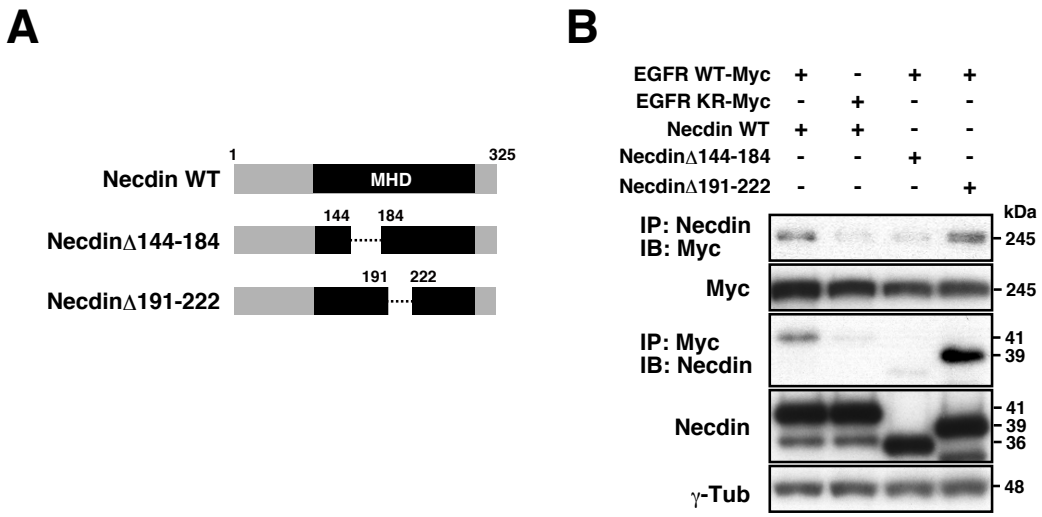

Figure III.23 EGFR binding activities of necdin deletion mutants.
(**A**) Diagrams of wild-type necdin (Necdin WT) and its deletion mutants. The necdin deletion mutants (NecdinΔ144-184, NecdinΔ191-222) reported previously (Taniura et al., 2005) were examined for the EGFR-binding activity. MHD, MAGE homology domain. (**B**) HEK293A cells were transfected with cDNAs for Myc-tagged EGFR, EGFR KR, necdin, and its mutants. Cell lysates were immunoprecipitated (IP) with antibodies to necdin and Myc, and immunoblotted (IB) for Myc, necdin, and γ-tubulin (γ-Tub) as in **Fig. 4B**.

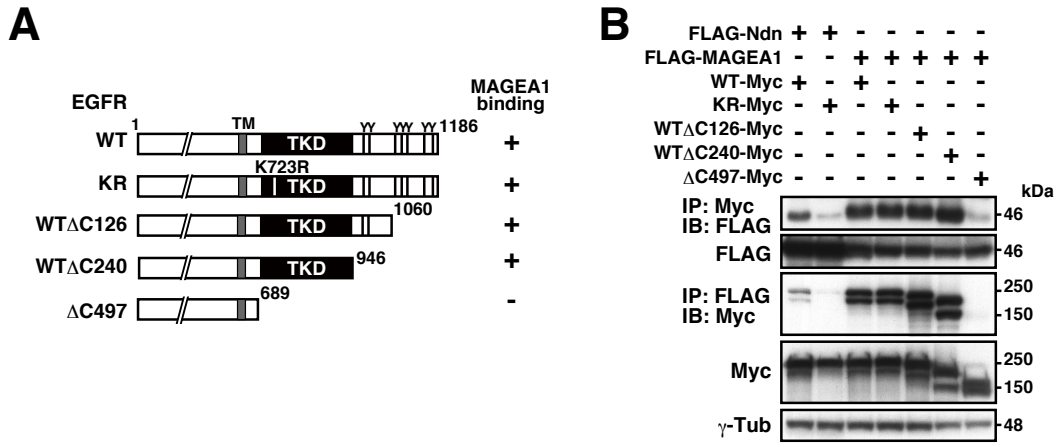

Figure III.24 MAGEA1 interacts with EGFR in an autophosphorylation independent manner.

(**A**) Diagrams of EGFR and its C-terminal-truncated mutants. WT, wild-type; KR, K723R mutant; ΔC126, C-terminal 126 residue deletion; ΔC240, C-terminal 240 residue deletion; ΔC497, C-terminal 497 residue deletion; TM, transmembrane domain; TKD, tyrosine kinase domain; Y, autophosphorylated tyrosine residues.

(**B**) HEK293A cells were co-transfected with cDNAs for Myc-tagged EGFR mutants, FLAG-tagged necdin (positive control) and FLAG-tagged MAGEA1. Cell lysates were immunoprecipitated (IP) with antibodies to Myc and FLAG, and immunoblotted (IB) for FLAG, Myc, and γ-tubulin (γ-Tub). Results are shown in ***A***.

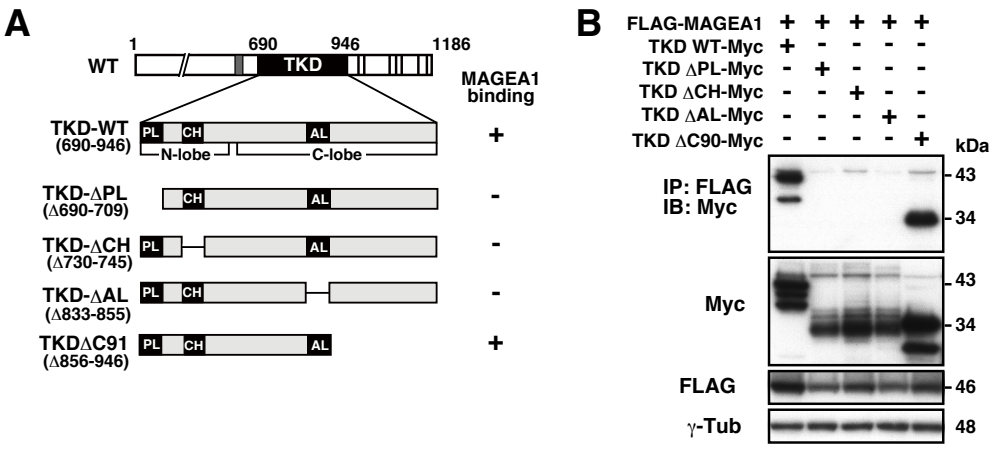

Figure III.25 MAGEA1 interacts with the tyrosine kinase domain.

(**A**) Diagrams of TKD deletion mutants. TKD-WT, wild-type TKD; TKDΔPL, phosphate-binding loop deletion; TKDΔCH, C-helix deletion; TKDΔAL, activation loop deletion; TKDΔC91, C-terminal 91 residue deletion. (**B**) Coimmunoprecipitation assay for TKD-deletion mutants. HEK293A cells were co-transfected with cDNAs for Myc-tagged TKD mutants and FLAG-tagged MAGEA1. Cell lysates were immunoprecipitated (IP) with antibodies to FLAG and immunoblotted (IB) for Myc, FLAG, and γ-tubulin (γ-Tub). Results are shown in **A**.

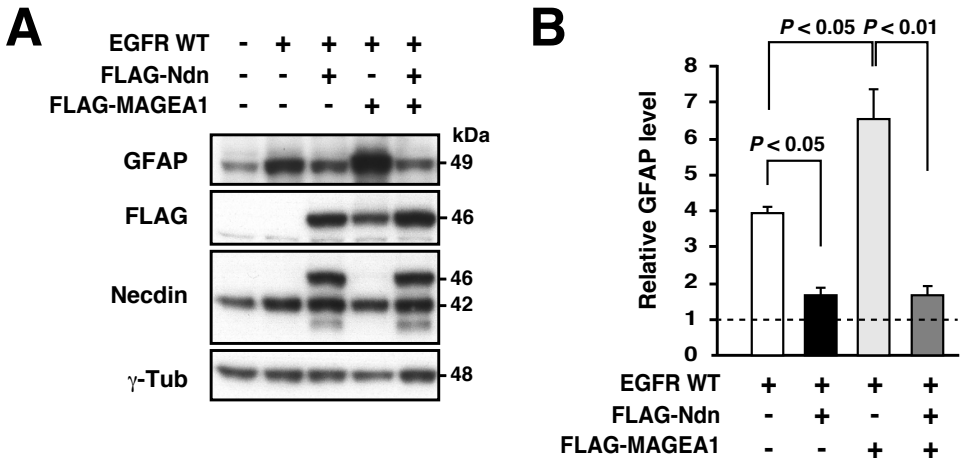

Figure III.26 MAGEA1 enhances EGFR-induced GFAP expression in primary CPCs.

(**A, B**) Effects of necdin and MAGEA1 on EGFR-induced GFAP expression. CPCs were transfected with combinations of cDNAs for EGFR, FLAG-Ndn and FLAG-MAGEA1. GFAP expression in transfected CPCs was analyzed immunoblotting (**A**) and quantified by densitometry (**B**). FLAG-tagged and endogenous necdin proteins are detected at 46 and 42 kDa, respectively. The broken line indicates the basal GFAP level in CPCs expressing td-Tomato alone (=1). Each value represents the mean ± SEM, $n = 3$. *P*-values were calculated using one-way ANOVA followed by Tukey-Kramer *post hoc* test.

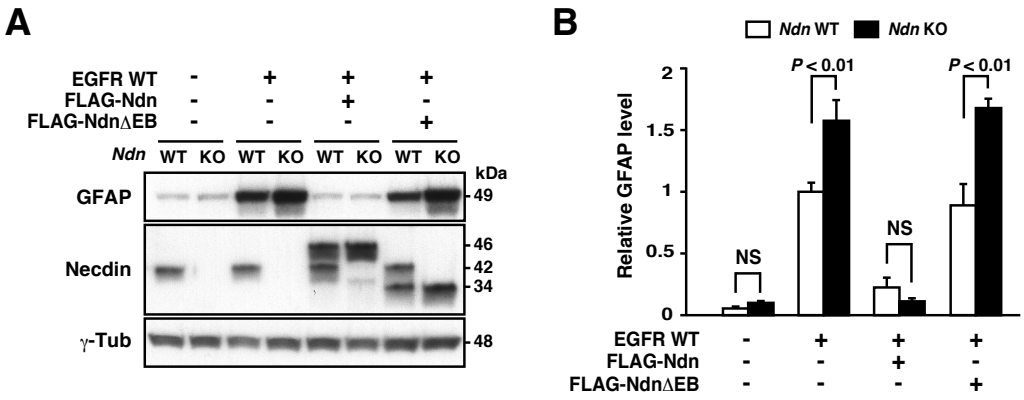

Figure III.27 The increase in the GFAP level was completely suppressed by coexpression of necdin, but not of necdinΔEB.

(**A**, **B**) Effect of endogenous necdin on GFAP expression induced by EGFR overexpression. CPCs prepared from wild-type (*Ndn* WT) and necdin-null (*Ndn* KO) mice at E14.5 were transfected with EGFR, FLAG-necdin (Ndn) and NdnΔEB, and GFAP expression levels were analyzed. Each value represents the mean ± SEM, $n = 4$. *P*-values were calculated using one-way ANOVA followed by Tukey-Kramer *post hoc* test. NS, not significant at $P \geq 0.05$.

IV. DISCUSSION

IV-1. RAS/MEK/ERK signaling pathway and gliogenesis

EGFR signaling in CPCs plays an important role in astrocyte differentiation during the late embryonic period when the transition from neurogenesis to gliogenesis occurs in developing cortex (Temple, 2001). CPCs show little or no reactivity to EGF at early stages of embryonic cortical development (Tropepe et al., 1999; Qian et al, 2000; Zhu and Parada, 2002; Gritti et al., 1999). As the development proceeds, the bFGF level becomes high and induces EGFR expression in CPCs (Qian et al., 1997; Powell et al., 1991). Mice lacking EGFR develop a progressive neurodegeneration and defect in cortical astrocytes (Wagner et al., 2006). Furthermore, the RAS/ERK signaling pathway is involved in astrocyte differentiation during brain development (Dasgupta and Gutmann, 2005; Li et al., 2014; Li et al., 2012; Wang et al., 2012). These findings indicate that the RAS/MEK/ERK signaling pathway is involved in the control of astrocyte differentiation during cortical development. Necdin suppresses the EGFR/ERK signaling pathway by interacting with autophosphorylated EGFR in EGF-responsive CPCs. Furthermore, the EGFR-inducible immediate early gene IEX-1 (also known as IER3) induces astrocyte differentiation in human glioma cells (You et al., 2007). In the present study, IEX1 mRNA and GFAP expression levels increase significantly in EGF-treated necdin-null CPCs. Thus, we propose that necdin is an intrinsic suppressor of the EGF/EGFR signaling in CPCs to restrict astrocyte differentiation during the late period of cortical development.

IV-2. Structural changes of inactive and active EGFR

Stimulation of EGFR by EGF induces autophosphorylation of the C-tail followed by activation of downstream signaling pathways including the RAS/MEK/ERK and PI3K/Akt cascades (Jorissen et al., 2003). Activation of EGFR induces conformational changes of the ATP binding pocket between the N-lobe and the C-lobe in the TKD core region. The conformational change from "close" to "open" status is regulated by C-helix movement, which is coupled with the motions of the juxtamembrane segment that connects the transmembrane helix to the TKD and the C-tail segment (Jura et al., 2009; Mustafa et al., 2011). This may allosterically control the autophosphorylation of the C-tail. Necdin suppresses the EGFR/ERK signal transduction by interacting with the C-terminal region of the TKD. Necdin interacts with the TKD of EGFR only in its activated state, and the interaction is enhanced in the absence of the C-tail. This suggests that the unphosphorylated C-tail interferes with the interaction between necdin and the TKD (**Fig IV.1**). This idea is supported by the previous observations on the conformational changes of the C-tail and TKD in inactive and active states of EGFR (Jura et al., 2009; Mustafa et al., 2011). We speculate that necdin binds to the TKD when autophosphorylation of the C-tail uncovers the necdin-binding site on the TKD (**Fig IV.2A,B**). Thus, the C-tail may serve as a molecular switch to control the interaction between necdin and the TKD in CPCs.

IV-3. Difference between necdin and MIG6

The TKD of EGFR consists of N-terminal (N-lobe) and C-terminal (C-lobe) regions, and the N-lobe contains the specific sites for the tyrosine kinase activity such as ATP-binding site, C-helix, and phosphate-binding loop (P-loop) (Lemmon et al., 2014;

Zhang et al., 2006) (**Fig IV.2A)**. Necdin binds to the C-terminal end of the C-lobe, and this location may be critical for the reduced interaction between autophosphorylated C-tail and Grb2 without affecting the tyrosine kinase activity. Intriguingly, the EGFR feedback inhibitor MIG6 (also known as RALT or ERRFI1), like necdin, binds to the TKD when EGFR is activated (Zhang et al., 2007). However, MIG6, unlike necdin, is transiently expressed by EGFR ligands and inhibits the tyrosine kinase activity to suppress both RAS/ERK and PI3K/Akt pathways (Segatto et al., 2011). This may be attributable to the structural characteristics of MIG6 associated with the allosteric control of the EGFR kinase activity (Anastasi et al., 2007; Zhang et al., 2007). The differences between necdin and MIG6 imply that necdin is a unique inhibitor of the EGFR/RAS/ERK signaling pathway linked to cellular proliferation but not of the PI3K/Akt signaling pathway linked to cell survival. These findings are consistent with the notion that necdin suppresses cell proliferation and maintains cell survival.

IV-4. Neurogenesis and gliogenesis in cortical development

Neural precursor cells in the embryonic forebrain of necdin-null mice are highly proliferative *in vivo* during the early period of development when neurogenesis occurs actively (Huang et al., 2013; Minamide et al., 2014). Necdin suppresses the proliferation of CPCs by increasing p16 expression through interaction with the *p16* transcriptional repressor Bmi1 and by reducing *Cdk1* expression through interaction with the *Cdk1* transcriptional activator E2F1 (Minamide et al., 2014), suggesting that necdin prevents hyperproliferation of early CPCs, which are competent to differentiate into neurons, by modulating the activities of these cell cycle regulatory proteins. The present study provides evidence that necdin suppresses astrocyte generation from EGF-responsive

CPCs through attenuation of the EGFR/ERK pathway. Thus, necdin may control the EGFR/ERK signaling pathway in late CPCs, which are competent to differentiate into astrocytes. We propose that necdin fine-tunes the regulatory systems involved in neurogenesis and gliogenesis at different stages of normal cortical development.

IV-5. Implication in cancer pathogenesis

Numerous studies have indicated that EGFR signaling is central to the pathogenesis of many cancers such as glioblastoma, breast cancer and non-small-cell lung cancer (NSCLC), in which genetic alterations of EGFR such as gene amplification and mutations may be involved (Normanno et al., 2006; Sibilia et al., 2007). Furthermore, the importance of EGFR signaling in cancer progression is supported by the fact that several anticancer drugs such as gefitinib and erlotinib target the EGFR TKD (Herbst et al., 2004). The present study has clarified that necdin acts as an endogenous suppressor of EGFR signaling. Furthermore, necdin is not expressed in many cancer cells, where the necdin gene is hypermethylated and mutated (De Faveri et al., 2013). These findings raise the possibility that necdin potentially suppresses malignant transformation induced by increased EGFR signaling in various types of cancers. As shown in this study, necdin suppresses EGFR overexpression-induced astrocyte differentiation, whereas MAGEA1, another MAGE family member expressed in many kinds of malignant tumors (Chomez et al., 2001), promotes it, suggesting that necdin and MAGEA1 exert opposite effects on EGFR-mediated signaling events. Thus, it is tempting to speculate that these different types of MAGE family members antagonistically control malignant transformation induced by EGFR or its mutants.

IV-6. Implication in gliomagenesis

Dysregulation of EGFR signal transduction has been suggested to contribute to the etiology of brain tumors including gliomas (Nicholas et al., 2006). Aberrant activation of the RAS/MEK/ERK pathway is also involved in the pathogenesis of astrocytoma or glioma (Li et al., 2014; Zhu and Parada, 2002). On the other hand, necdin is not expressed in many cell lines derived from neural cell-derived tumors such as glioma, neuroblastoma, pheochromocytoma, and ependymoma (Aizawa et al., 2011; Aizawa et al., 1992; Kobayashi et al., 2002). A network modeling study of DNA copy number aberrations implicates necdin in suppressing cell growth of glioblastomas (Jornsten et al., 2011). Furthermore, reduced *NDN* expression in low grade gliomas strongly correlates with reduced overall survival of patients with gliomas (Li et al., 2015). The gene overexpression experiments demonstrated that necdin strongly prevents astrocyte differentiation induced by overexpression of wild-type EGFR or its mutant equivalent to human EGFR variant III (EGFRvIII) in CPCs. Overexpression of EGFR and its deletion mutants such as EGFRvIII is commonly found in glioblastomas (Nicholas et al., 2006). Gliomas are proposed to arise from neural stem cells that are generated from glial progenitor cells or astrocytes via reprogrammed processes (Sanai et al., 2005; Zhu and Parada, 2002). Thus, we infer that necdin serves as a tumor suppressor that controls the EGFR/ERK pathway in astrocyte progenitors to prevent their malignant transformation.

IV-7. Implication in pathogenesis of Prader-Willi syndrome

The human necdin gene (*NDN*) is located in chromosome 15q11.2-q12 (Nakada et al., 1998), a region deleted in Prader-Willi syndrome (PWS), a typical genomic

imprinting-associated neurodevelopmental disorder. *NDN* is maternally imprinted, expressed only from the paternal allele, and not expressed in individuals with PWS (Jay et al., 1997; MacDonald and Wevrick, 1997). Although patients with PWS exhibit symptoms due to hypothalamic abnormalities such as hyperphagia and hypogonadism, there is limited information on neuropathological lesions in PWS. In contrast, the mouse necdin gene (*Ndn*) located in chromosome 7C is also imprinted, and paternal *Ndn*-mutant mice display failure-to-thrive and early neonatal lethality (Gérard et al., 1999; Muscatelli et al., 2000). Moreover, PWS model mice created by transgene insertion or PWS imprinting-center mutation fail to express necdin and display early postnatal lethality (Gabriel et al., 1999; Yang et al., 1998). The *Ndn*-mutant mice, mostly examined at their embryonic and neonatal stages, exhibit various morphological and functional abnormalities, in which several are reminiscent of PWS (Aebischer et al., 2011; Bush and Wevrick, 2010, 2012; Fujiwara et al., 2012; Hasegawa et al., 2012; Kuwajima et al., 2010; Kuwajima et al., 2006; Kuwako et al., 2005; Miller et al., 2009; Muscatelli et al., 2000; Ren et al., 2003; Tennese et al., 2008; Zanella et al., 2008). Thus, primary cells such as CPCs prepared from necdin-null mice are indispensable for dissecting molecular mechanisms underlying these abnormalities. We assume that other stem/progenitor cells expressing both necdin and EGFR also exhibit enhanced EGFR signaling in the absence of endogenous necdin. The present findings warrant close examination of the pathologies associated with dysregulation of EGFR signaling in PWS.

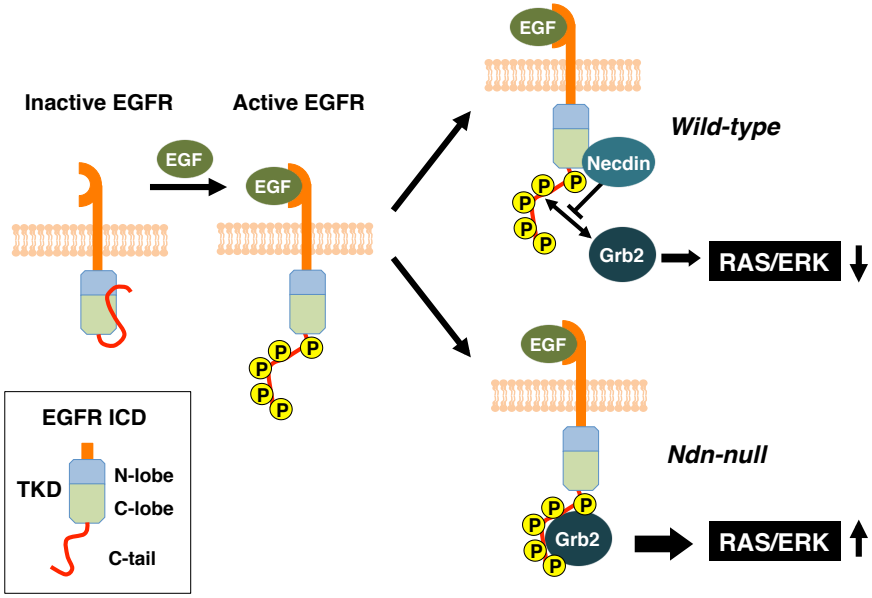

Figure IV.1 A schematic model for suppression of EGFR signaling by necdin.

Necdin binds to EGF-activated EGFR via the TKD C-lobe and blocks the interaction between EGFR and Grb2, resulting in the suppression of the RAS/ERK signaling pathway. For details, see Discussion. ICD, intracellular domain; TKD, tyrosine kinase domain; P, phospho-tyrosine; Ndn+, wild-type necdin; Ndn-, necdin deficiency.

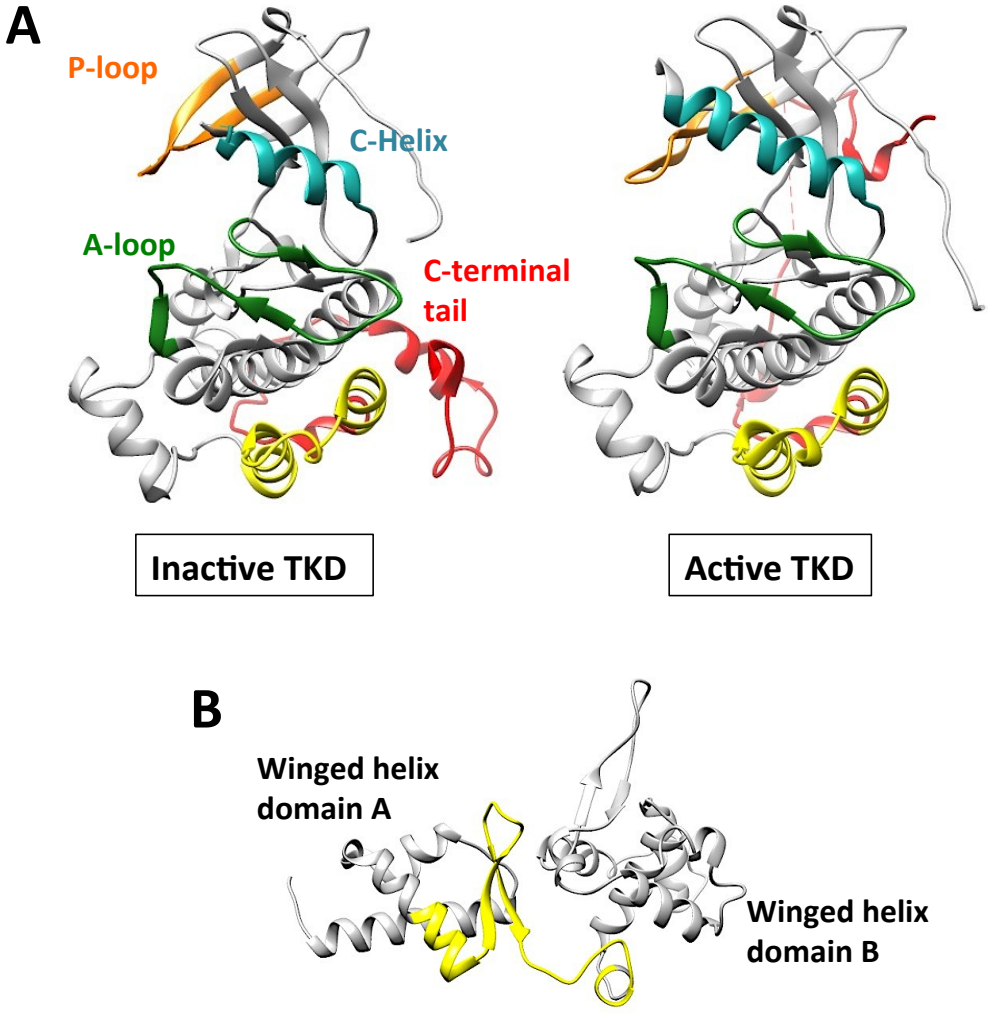

Figure IV.2 Ribbon representation of the crystalized conformations of EGFR TKD and predicted structure of necdin MHD.
(A) Crystal structures of inactive EGFR TKD (PDB 4G5J)(left) and active EGFR TKD in complex with ATP analog-peptide (PDB 2GS6)(right). Yellow; necdin-binding region. **(B)** A predicted necdin MHD structure. The structural model was predicted on the basis of structural data of necdin-like 2 (PDB 3NW0) by the Spanner program and presented by UCSF Chimera. Yellow; EGFR-binding region.

CONCLUSIONS

- EGFR and necdin are coexpressed in primary CPCs.
- Necdin binds to autophosphorylated EGFR via its tyrosine kinase domain.
- The EGFR/ERK pathway is activated in necdin-null CPCs through increased interaction between EGFR and Grb2.
- EGF-promoted astrocyte differentiation is accelerated via the EGFR/ERK pathway in necdin-null CPCs.
- Necdin restrains astrocyte differentiation induced by overexpression of EGFR or its EGF binding-defective mutant in CPCs.
- Necdin is an intrinsic suppressor of EGFR/ERK signaling in CPCs under physiological and pathological conditions.

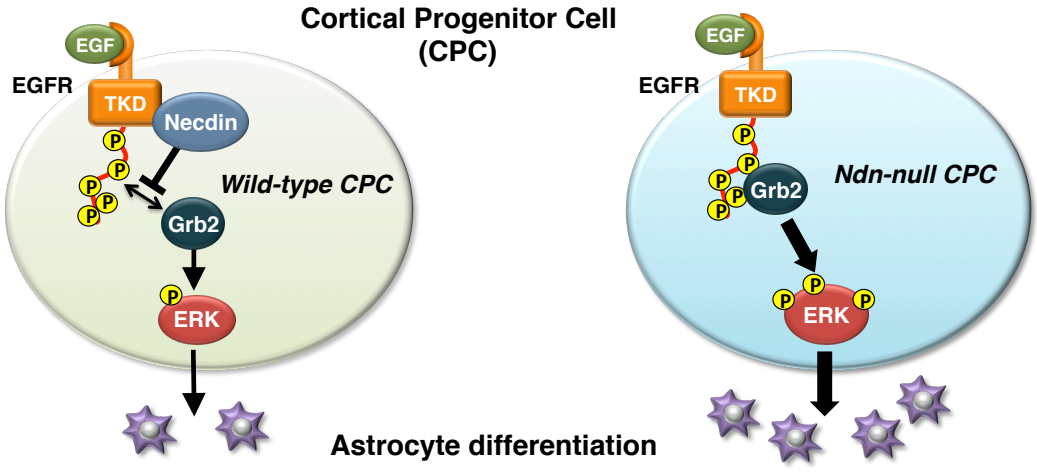

VII. REFERENCES

Acconcia F, Sigismund S, Polo S, Ubiquitin in trafficking: the network at work, Exp Cell Res 315 (2009) 1610-1618.

Aebischer J, Sturny R, Andrieu D, Rieusset A, Schaller F, Geib S, Raoul C, Muscatelli F, Necdin protects embryonic motoneurons from programmed cell death, PLoS One 6 (2011) e23764.

Aizawa T, Hasegawa K, Ohkumo T, Haga S, Ikeda K, Yoshikawa K, Neural stem cell-like gene expression in a mouse ependymoma cell line transformed by human BK polyomavirus, Cancer Sci 102 (2011) 122-129.

Aizawa T, Maruyama K, Kondo H, Yoshikawa K, Expression of necdin, an embryonal carcinoma-derived nuclear protein, in developing mouse brain, Brain Res Dev Brain Res 68 (1992) 265-274.

Anastasi S, Fiorentino L, Fiorini M, Fraioli R, Sala G, Castellani L, Alemà S, Alimandi M, Segatto O, Feedback inhibition by RALT controls signal output by the ErbB network, Oncogene 22 (2003) 4221-4234.

Anastasi S, Baietti MF, Frosi Y, Alema S, Segatto O, The evolutionarily conserved EBR module of RALT/MIG6 mediates suppression of the EGFR catalytic activity, Oncogene 26 (2007) 7833-7846.

Barker PA, Salehi A, The MAGE proteins: emerging roles in cell cycle progression, apoptosis, and neurogenetic disease, J Neurosci Res 67 (2002) 705-712.

Barnabe-Heider F, Wasylnka JA, Fernandes KJ, Porsche C, Sendtner M, Kaplan DR, Miller FD, Evidence that embryonic neurons regulate the onset of cortical gliogenesis via cardiotrophin-1, Neuron 48 (2005) 253-265.

Batzer AZ, Rotin D, Ureña JM, Skolnik EY, Schlessinger J, Hierarchy of binding sites for Grb2 and Shc on the epidermal growth factor receptor, Mol Cell Biol 14 (1994) 5192-5201.

Biscardi JS, Maa MC, Tice DA, Cox ME, Leu TH, Parsons SJ, c-Src-mediated phosphorylation of the epidermal growth factor receptor on Tyr845 and Tyr1101 is associated with modulation of receptor function, J Biol Chem 274 (1999) 8335-8343.

Bonni A, Sun Y, Nadal-Vicens M, Bhatt A, Frank DA, Rozovsky I, Stahl N, Yancopoulos GD, Greenberg ME, Regulation of gliogenesis in the central nervous system by the JAK-STAT signaling pathway, Science 278 (1997) 477-483.

Brunelli S, Tagliafico E, De Angelis FG, Tonlorenzi R, Baesso S, Ferrari S, Niinobe M,

Yoshikawa K, Schwartz RJ, Bozzoni I, Ferrari S, Cossu G, Msx2 and necdin combined activities are required for smooth muscle differentiation in mesoangioblast stem cells, Circ Res 94 (2004) 1571-1578.

Burrows RC, Wancio D, Levitt P, Lillien L, Response diversity and the timing of progenitor cell maturation are regulated by developmental changes in EGFR expression in the cortex, Neuron 19 (1997) 251-267.

Bush JR, Wevrick R, Loss of Necdin impairs myosin activation and delays cell polarization, Genesis 48 (2010) 540-553.

Bush JR, Wevrick R, Loss of the Prader-Willi obesity syndrome protein necdin promotes adipogenesis, Gene 497 (2012) 45-51.

Chomez P, De Backer O, Bertrand M, De Plaen E, Boon T, Lucas S, An overview of the MAGE gene family with the identification of all human members of the family, Cancer Res 61 (2001) 5544-5551.

Dasgupta B, Gutmann, DH, Neurofibromin regulates neural stem cell proliferation, survival, and astroglial differentiation in vitro and in vivo, J Neurosci 25 (2005) 5584-5594.

De Faveri LE, Hurst CD, Platt FM, Taylor CF, Roulson JA, Sanchez-Carbayo M, Knowles MA, Chapman EJ, Putative tumour suppressor gene necdin is hypermethylated and mutated in human cancer, Br J Cancer 108 (2013) 1368-1377.

de Melker AA, van der Horst G, Calafat J, Jansen H, Borst J, c-Cbl ubiquitinates the EGF receptor at the plasma membrane and remains receptor associated throughout the endocytic route, J Cell Sci 114 (2001) 2167-2178.

Deribe YL, Wild P, Chandrashaker A, Curak J, Schmidt MH, Kalaidzidis Y, Milutinovic N, Kratchmarova I, Buerkle L, Fetchko MJ, Schmidt P, Kittanakom S, Brown KR, Jurisica I, Blagoev B, Zerial M, Stagljar I, Dikic I, Regulation of epidermal growth factor receptor trafficking by lysine deacetylase HDAC6, Sci Signal 2 (2009) ra84.

Derynck R, Roberts AB, Winkler ME, Chen EY, Goeddel DV, Human transforming growth factor-alpha: precursor structure and expression in E.Coli, Cell 38 (1984) 287-297.

Dikic I, Giordano S, Negative receptor signalling, Curr Opin Cell Biol 15 (2003) 128-135.

Ewald JA, Coker KJ, Price JO, Staros JV, Guyer CA, Stimulation of mitogenic pathways through kinase-impaired mutations of the epidermal growth factor receptor, Exp Cell Res 268 (2001) 262-273.

Frosi Y, Anastasi S, Ballarò C, Varsano G, Castellani L, Maspero E, Polo S, Alemà S, Segatto O, A two-tiered mechanism of EGFR inhibition by RALT/MIG6 via kinase suppression and receptor degradation, J Cell Biol 189 (2010) 557-571.

Fujiwara K, Hasegawa K, Ohkumo T, Miyoshi H, Tseng YH, Yoshikawa K, Necdin controls proliferation of white adipocyte progenitor cells, PLoS One 7 (2012) e30948.

Gabriel JM, Merchant M, Ohta T, Ji Y, Caldwell RG, Ramsey MJ, Tucker JD, Longnecker R, Nicholls RD, A transgene insertion creating a heritable chromosome deletion mouse model of Prader-Willi and Angelman syndromes, Proc Natl Acad Sci USA 96 (1999) 9258-9263.

Gérard M, Hernandez L, Wevrick R, Stewart CL, Disruption of the mouse necdin gene results in early post-natal lethality, Nat Genet 23 (1999) 199-202.

Gritti A, Frölichsthal-Schoeller P, Galli R, Parati EA, Cova L, Pagano SF, Bjornson CR, Vescovi AL, Epidermal and fibroblast growth factors behave as mitogenic regulators for a single multipotent stem cell-like population from the subventricular region of the adult mouse forebrain, J Neurosci 19 (1999) 3287-3297.

Gur G, Rubin C, Katz M, Amit I, Citri A, Nilsson J, Amariglio N, Henriksson R, Rechavi G, Hedman H, Wides R, Yarden Y, LRIG1 restricts growth factor signaling by enhancing receptor ubiquitylation and degradation, EMBO J 23 (2004) 3270-3281.

Gur I, Fujiwara K, Hasegawa K, Yoshikawa K, Necdin promotes ubiquitin-dependent degradation of PIAS1 SUMO E3 ligase, PLoS One 9 (2014) e99503.

Haglund K, Sigismund S, Polo S, Szymkiewicz I, Di Fiore PP, Dikic I, Multiple monoubiquitination of RTKs is sufficient for their endocytosis and degradation, Nat Cell Biol 5 (2003) 461-466.

Hasegawa K, Yoshikawa K, Necdin regulates p53 acetylation via Sirtuin1 to modulate DNA damage response in cortical neurons, J Neurosci 28 (2008) 8772-8784.

Hasegawa K, Kawahara T, Fujiwara K, Shimpuku M, Sasaki T, Kitamura T, Yoshikawa K, Necdin controls FoxO1 acetylation in hypothalamic arcuate neurons to modulate the thyroid axis, J Neurosci 32 (2012) 5562-5572.

Hayashi Y, Matsuyama K, Takagi K, Sugiura H, Yoshikawa K, Arrest of cell growth by necdin, a nuclear protein expressed in postmitotic neurons, Biochem Biophys Res Commun 213 (1995) 317-324.

Herbst RS, Fukuoka M, Baselga J, Gefitinib--a novel targeted approach to treating cancer, Nat Rev Cancer 4 (2004) 956-965.

Higashiyama S, Horikawa M, Yamada K, Ichino N, Nakano N, Nakagawa T, Miyagawa J, Matsushita N, Nagatsu T, Taniguchi N, Ishiguro H, A novel brain-derived member of

the epidermal growth factor family that interacts with ErbB3 and ErbB4, J Biochem 122 (1997) 675-680.

Holbro T, Hynes NE, ErbB receptors: directing key signaling networks throughout life, Annu Rev Pharmacol Toxicol 44 (2004) 195-217.

Huang Z, Fujiwara K, Minamide R, Hasegawa K, Yoshikawa K, Necdin controls proliferation and apoptosis of embryonic neural stem cells in an oxygen tension-dependent manner, J Neurosci 33 (2013) 10362-10373.

Hu B, Wang S, Zhang Y, Feghali CA, Dingman JR, Wright TM, A nuclear target for interleukin-1alpha: interaction with the growth suppressor necdin modulates proliferation and collagen expression, Proc Natl Acad Sci USA 100 (2003) 10008-10013.

Humphrey PA, Wong AJ, Vogelstein B, Friedman HS, Werner MH, Bigner DD, Bigner SH, Amplification and expression of the epidermal growth factor receptor gene in human glioma xenografts, Cancer Res 48 (1988) 2231-2238.

Hynes NE, Lane HA, ERBB receptors and cancer: the complexity of targeted inhibitors, Nat Rev Cancer 5 (2005) 341-354.

Jay P, Rougeulle C, Massacrier A, Moncla A, Mattei MG, Malzac P, Roeckel N, Taviaux S, Lefranc JL, Cau P, Berta P, Lalande M, Muscatelli F, The human necdin gene, NDN, is maternally imprinted and located in the Prader-Willi syndrome chromosomal region, Nat Genet 17 (1997) 357-361.

Johe KK, Hazel TG, Muller T, Dugich-Djordjevic MM, McKay RD, Single factors direct the differentiation of stem cells from the fetal and adult central nervous system, Genes Dev 10 (1996) 3129-3140.

Jorissen RN, Walker F, Pouliot N, Garrett TP, Ward CW, Burgess AW, Epidermal growth factor receptor: mechanisms of activation and signalling, Exp Cell Res 284 (2003) 31-53.

Jornsten R, Abenius T, Kling T, Schmidt L, Johansson E, Nordling TE, Nordlander B, Sander C, Gennemark P, Funa K, Nilsson B, Lindahl L, Nelander S, Network modeling of the transcriptional effects of copy number aberrations in glioblastoma, Mol Syst Biol 7 (2011) 486.

Jungbluth AA, Stockert E, Huang HJ, Collins VP, Coplan K, Iversen K, Kolb D, Johns TJ, Scott AM, Gullick WJ, Ritter G, Cohen L, Scanlan MJ, Cavenee WK, Old LJ, A monoclonal antibody recognizing human cancers with amplification/overexpression of the human epidermal growth factor receptor, Proc Natl Acad Sci USA 100 (2003) 639-644.

Jura N, Endres NF, Engel K, Deindl S, Das R, Lamers MH, Wemmer DE, Zhang X,

Kuriyan J, Mechanism for activation of the EGF receptor catalytic domain by the juxtamembrane segment, Cell 137 (2009) 1293-1307.

Kario E, Marmor MD, Adamsky K, Citri A, Amit I, Amariglio N, Rechavi G, Yarden Y, Suppressors of cytokine signaling 4 and 5 regulate epidermal growth factor receptor signaling, J Biol Chem 280 (2005) 7038-7048.

Kilpatrick TJ, Bartlett PF, Cloned multipotential precursors from the mouse cerebrum require FGF-2, whereas glial restricted precursors are stimulated with either FGF-2 or EGF, J Neurosci 15 (1995) 3653-3661.

Kobayashi M, Taniura H, Yoshikawa K, Ectopic expression of necdin induces differentiation of mouse neuroblastoma cells, J Biol Chem 277 (2002) 42128-42135.

Kumar A, Petri ET, Halmos B, Boggon TJ, Structure and clinical relevance of the epidermal growth factor receptor in human cancer, J Clin Oncol 26 (2008) 1742-1751.

Kuwajima T, Hasegawa K, Yoshikawa K, Necdin promotes tangential migration of neocortical interneurons from basal forebrain, J Neurosci 30 (2010) 3709-3714.

Kuwajima T, Nishimura I, Yoshikawa K, Necdin promotes GABAergic neuron differentiation in cooperation with Dlx homeodomain proteins, J Neurosci 26 (2006) 5383-5392.

Kuwajima T, Taniura H, Nishimura I, Yoshikawa K, Necdin interacts with the Msx2 homeodomain protein via MAGE-D1 to promote myogenic differentiation of C2C12 cells, J Biol Chem 279 (2004) 40484-40493.

Kuwako K, Hosokawa A, Nishimura I, Uetsuki T, Yamada M, Nada S, Okada M, Yoshikawa K, Disruption of the paternal necdin gene diminishes TrkA signaling for sensory neuron survival, J Neurosci 25 (2005) 7090-7099.

Kuwako K, Taniura H, Yoshikawa K, Necdin-related MAGE proteins differentially interact with the E2F1 transcription factor and the p75 neurotrophin receptor, J Biol Chem 279 (2004) 1703-1712.

Lemmon MA, Schlessinger J, Ferguson KM, The EGFR family: not so prototypical receptor tyrosine kinases, Cold Spring Harb Perspect Biol 6 (2014) a020768.

Lee S, Walker CL, Karten B, Kuny SL, Tennese AA, O'Neill MA, Wevrick R, Essential role for the Prader-Willi syndrome protein necdin in axonal outgrowth, Hum Mol Genet 14 (2005) 627-637.

Lillien L, Raphael H, BMP and FGF regulate the development of EGF-responsive neural progenitor cells, Development 127 (2000) 4993-5005.

Li S, Mattar P, Dixit R, Lawn SO, Wilkinson G, Kinch C, Eisenstat D, Kurrasch DM,

Chan JA, Schuurmans C, RAS/ERK signaling controls proneural genetic programs in cortical development and gliomagenesis, J Neurosci 34 (2014) 2169-2190.

Li X, Hughes SC, Wevrick R, Evaluation of melanoma antigen (MAGE) gene expression in human cancers using The Cancer Genome Atlas, Cancer Genet 208 (2015) 25-34.

Li X, Newbern JM, Wu Y, Morgan-Smith M, Zhong J, Charron J, Snider WD, MEK is a key regulator of gliogenesis in the developing brain, Neuron 75 (2012) 1035-1050.

MacDonald HR, Wevrick R, The necdin gene is deleted in Prader-Willi syndrome and is imprinted in human and mouse, Hum Mol Genet 6 (1997) 1873-1878.

Madshus IH, Stang E, Internalization and intracellular sorting of the EGF receptor: a model for understanding the mechanisms of receptor trafficking, J Cell Sci 122 (2009) 3433-3439.

Maric D, Maric I, Chang YH, Barker JL, Prospective cell sorting of embryonic rat neural stem cells and neuronal and glial progenitors reveals selective effects of basic fibroblast growth factor and epidermal growth factor on self-renewal and differentiation, J Neurosci 23 (2003) 240-251.

Maruyama K, Usami M, Aizawa T, Yoshikawa K, A novel brain-specific mRNA encoding nuclear protein (necdin) expressed in neurally differentiated embryonal carcinoma cells, Biochem Biophys Res Commun 178 (1991) 291-296.

Miller NL, Wevrick R, Mellon PL, Necdin, a Prader-Willi syndrome candidate gene, regulates gonadotropin-releasing hormone neurons during development, Hum Mol Genet 18 (2009) 248-260.

Minamide R, Fujiwara K, Hasegawa K, Yoshikawa K, Antagonistic interplay between necdin and Bmi1 controls proliferation of neural precursor cells in the embryonic mouse neocortex, PLoS One 9 (2014) e84460.

Mosesson Y, Shtiegman K, Katz M, Zwang Y, Vereb G, Szollosi J, Yarden Y, Endocytosis of receptor tyrosine kinases is driven by monoubiquitylation, not polyubiquitylation, J Biol Chem 278 (2003) 21323-21326.

Muscatelli F, Abrous DN, Massacrier A, Boccaccio I, Le Moal M, Cau P, Cremer H, Disruption of the mouse Necdin gene results in hypothalamic and behavioral alterations reminiscent of the human Prader-Willi syndrome, Hum Mol Genet 9 (2000) 3101-3110.

Mustafa M, Mirza A, Kannan N, Conformational regulation of the EGFR kinase core by the juxtamembrane and C-terminal tail: a molecular dynamics study, Proteins 79 (2011) 99-114.

Nakada Y, Taniura H, Uetsuki T, Inazawa J, Yoshikawa K, The human chromosomal

gene for necdin, a neuronal growth suppressor, in the Prader-Willi syndrome deletion region, Gene 213 (1998) 65-72.

Nakashima K, Wiese S, Yanagisawa M, Arakawa H, Kimura N, Hisatsune T, Yoshida K, Kishimoto T, Sendtner M, Taga T, Developmental requirement of gp130 signaling in neuronal survival and astrocyte differentiation, J Neurosci 19 (1999) 5429-5434.

Nicholas MK, Lukas RV, Jafri NF, Faoro L, Salgia R, Epidermal growth factor receptor - mediated signal transduction in the development and therapy of gliomas, Clin Cancer Res 12 (2006) 7261-7270.

Nicholson SE, Metcalf D, Sprigg NS, Columbus R, Walker F, Silva A, Cary D, Willson TA, Zhang JG, Hilton DJ, Alexander WS, Nicola NA, Suppressor of cytokine signaling (SOCS)-5 is a potential negative regulator of epidermal growth factor signaling, Proc Natl Acad Sci USA 102 (2005) 2328-2333.

Nie W, Tang L, Zhang H, Shao J, Wang Y, Chen L, Li D, Guan X, Structural analysis of the EGFR TK domain and potential implications for EGFR targeted therapy, Int J Oncol 40 (2012) 1763-1769.

Normanno N, De Luca A, Bianco C, Strizzi L, Mancino M, Maiello MR, Carotenuto A, De Feo G, Caponigro F, Salomon DS, Epidermal growth factor receptor (EGFR) signaling in cancer, Gene 366 (2006) 2-16.

Novak U, Walker F, Kaye A, Expression of EGFR-family proteins in the brain: role in development, health and disease, J Clin Neurosci 8 (2001) 106-111.

Ochiai W, Yanagisawa M, Takizawa T, Nakashima K, Taga T, Astrocyte differentiation of fetal neuroepithelial cells involving cardiotrophin-1-induced activation of STAT3, Cytokine 14 (2001) 264-271.

Powell PP, Finklestein SP, Dionne CA, Jaye M, Klagsbrun M, Temporal, differential and regional expression of mRNA for basic fibroblast growth factor in the developing and adult rat brain, Brain Res Mol Brain Res 11 (1991) 71-77.

Plowman GD, Whitney GS, Neubauer MG, Green JM, McDonald VL, Todaro GJ, Shoyab M, Molecular cloning and expression of an additional epidermal growth factor receptor-related gene, Proc Natl Acad Sci USA 87 (1990) 4905-4909.

Qian X, Davis AA, SGoderie SK, Temple S, FGF2 concentration regulates the generation of neurons and glia from multipotent cortical stem cells, Neuron 18 (1997) 81-93.

Qian X, Shen Q, Goderie SK, He W, A. Capela, A.A. Davis, S. Temple, Timing of CNS cell generation: a programmed sequence of neuron and glial cell production from isolated murine cortical stem cells, Neuron 28 (2000) 69-80.

Ren J, Lee S, Pagliardini S, Gerard M, Stewart CL, Greer JJ, Wevrick R, Absence of Ndn, encoding the Prader-Willi syndrome-deleted gene necdin, results in congenital deficiency of central respiratory drive in neonatal mice, J Neurosci 23 (2003) 1569-1573.

Reynolds BA, Tetzlaff W, Weiss S, A multipotent EGF-responsive striatal embryonic progenitor cell produces neurons and astrocytes, J Neurosci 12 (1992) 4565-4574.

Sasada R, Ono Y, Taniyama Y, Shing Y, Folkman J, Igarashi K, Cloning and expression of cDNA encoding human betacellulin, a new member of the EGF family, Biochem Biophys Res Commun 190 (1993) 1173-1179.

Sanai N, Alvarez-Buylla A, Berger MS, Neural stem cells and the origin of gliomas, N Engl J Med 353 (2005) 811-822.

Schlessinger J, Ligand-induced, receptor-mediated dimerization and activation of EGF receptor, Cell 110 (2002) 669-672.

Segatto O, Anastasi S, Alemà S, Regulation of epidermal growth factor receptor signalling by inducible feedback inhibitors, J Cell Sci 124 (2011) 1785-1793.

Sibilia M, Kroismayr R, Lichtenberger BM, Natarajan A, Hecking M, Holcmann M, The epidermal growth factor receptor: from development to tumorigenesis, Differentiation 75 (2007) 770-787.

Sigismund S, Woelk T, Puri C, Maspero E, Tacchetti C, Transidico P, Di Fiore PP, Polo S, Clathrin-independent endocytosis of ubiquitinated cargos, Proc Natl Acad Sci USA 102 (2005) 2760-2765.

Sun Y, Goderie SK, Temple S, Asymmetric distribution of EGFR receptor during mitosis generates diverse CNS progenitor cells, Neuron 45 (2005) 873-886.

Taniguchi N, Taniura H, Niinobe M, Takayama C, Tominaga-Yoshino K, Ogura A, Yoshikawa K, The postmitotic growth suppressor necdin interacts with a calcium-binding protein (NEFA) in neuronal cytoplasm, J Biol Chem 275 (2000) 31674-31681.

Taniura H, Taniguchi N. Hara M, Yoshikawa K, Necdin, a postmitotic neuron-specific growth suppressor, interacts with viral transforming proteins and cellular transcription factor E2F1, J Biol Chem 273 (1998) 720-728.

Taniura H, Matsumoto K, Yoshikawa K, Physical and functional interactions of neuronal growth suppressor necdin with p53, J Biol Chem 274 (1999) 16242-16248.

Taniura H, Yoshikawa K, Necdin interacts with the ribonucleoprotein hnRNP U in the nuclear matrix, J Cell Biochem 84 (2002) 545-555.

Taniura H, Kobayashi M, Yoshikawa K, Functional domains of necdin for protein-protein interaction, nuclear matrix targeting, and cell growth suppression, J Cell Biochem 94 (2005) 804-815.

Temple S, The development of neural stem cells, Nature 414 (2001) 112-117.

Tennese AA, Gee CB, Wevrick R, Loss of the Prader-Willi syndrome protein necdin causes defective migration, axonal outgrowth, and survival of embryonic sympathetic neurons, Dev Dyn 237 (2008) 1935-1943.

Tice DA, Biscardi JS, Nickles AL, Parsons SJ, Mechanism of biological synergy between cellular Src and epidermal growth factor receptor, Proc Natl Acad Sci USA 96 (1999) 1415-1420.

Toyoda H, Komurasaki T, Uchida D, Morimoto S, Distribution of mRNA for human epiregulin, a differentially expressed member of the epidermal growth factor family, Biochem J 326 (1997) 69-75.

Tropepe V, Sibilia M, Ciruna BG, Rossant J, Wagner, E.F., van der Kooy, D., Distinct neural stem cells proliferate in response to EGF and FGF in the developing mouse telencephalon, Dev Biol 208 (1999) 166-188.

Uetsuki T, Takagi K, Sugiura H, Yoshikawa K, Structure and expression of the mouse necdin gene. Identification of a postmitotic neuron-restrictive core promoter, J Biol Chem 271 (1996) 918-924.

Viti J, Feathers A, Phillips J, Lillien L, Epidermal growth factor receptors control competence to interpret leukemia inhibitory factor as an astrocyte inducer in developing cortex, J Neurosci 23 (2003) 3385-3393.

Voldborg BR, Damstrup L, Spang-Thomsen M, Poulsen HS, Epidermal growth factor receptor (EGFR) and EGFR mutations, function and possible role in clinical trials, Ann Oncol 8 (1997) 1197-1206.

Wang Y, Kim E, Wang X, Novitch BG, Yoshikawa K, Chang LS, Zhu Y, ERK inhibition rescues defects in fate specification of Nf1-deficient neural progenitors and brain abnormalities, Cell 150 (2012) 816-830.

Wikstrand CJ, Hale LP, Batra SK, Hill ML, Humphrey PA, Kurpad SN, McLendon RE, Moscatello D, Pegram CN, Reist CJ, Monoclonal antibodies against EGFRvIII are tumor specific and react with breast and lung carcinomas and malignant gliomas, Cancer Res 55 (1995) 3140-3148.

Yamazaki H, Ohba Y, Tamaoki N, Shibuya M, A deletion mutation within the ligand binding domain is responsible for activation of epidermal growth factor receptor gene in human brain tumors, Jpn J Cancer Res 81 (1990) 773-779.

Yang T, Adamson TE, Resnick JL, Leff S, Wevrick R, Francke U, Jenkins NA, Copeland NG, Brannan CI, A mouse model for Prader-Willi syndrome imprinting-centre mutations, Nat Genet 19 (1998) 25-31.

Yarden Y, Sliwkowski MX, Untangling the ErbB signalling network, Nat Rev Mol Cell Biol 2 (2001) 127-137.

Yoshikawa K, Cell cycle regulators in neural stem cells and postmitotic neurons, Neurosci Res 37 (2000) 1-14.

You F, Osawa Y, Hayashi S, Nakashima S, Immediate early gene IEX-1 induces astrocytic differentiation of U87-MG human glioma cells, J Cell Biochem 100 (2007) 256-265.

Wagner B, Natarajan A, Grünaug S, Kroismayr R, Wagner EF, Sibilia M, Neuronal survival depends on EGFR signaling in cortical but not midbrain astrocytes, EMBO J 25 (2006) 752-762.

Woelk T, Oldrini B, Maspero E, Confalonieri S, Cavallaro E, Di Fiore PP, Polo S, Molecular mechanisms of coupled monoubiquitination, Nat Cell Biol 8 (2006) 1246-1254.

Zanella S, Watrin F, Mebarek S, Marly F, Roussel M, Gire C, Diene G, Tauber M, Muscatelli F, Hilaire G, Necdin plays a role in the serotonergic modulation of the mouse respiratory network: implication for Prader-Willi syndrome, J Neurosci 28 (2008) 1745-1755.

Zhang X, Gureasko J, Shen K, Cole PA, Kuriyan J, An allosteric mechanism for activation of the kinase domain of epidermal growth factor receptor, Cell 125 (2006) 1137-1149.

Zhang X, Pickin KA, Bose R, Jura N, Cole PA, Kuriyan J, Inhibition of the EGF receptor by binding of MIG6 to an activating kinase domain interface, Nature 450 (2007) 741-744.

Zhu Y, Parada LF, The molecular and genetic basis of neurological tumours, Nat Rev Cancer 2 (2002) 616-626.

VIII. ACKNOWLEDGEMENTS

I would like to express my sincere gratitude to Prof. Kazuaki Yoshikawa for his invaluable advices, discussion, and intimate encouragement. And I deeply appreciate his telling me to never give up and to enjoy researching.

I am especially grateful to Dr. Koichi Hasegawa for teaching me how to experiment, way of scientific thinking, and many scientific techniques. I would like to thank Dr. Kazushiro Fujiwara for his helpful advice and discussions. I would like to thank my collaborator, Dr. Masashi Yamada for helpful discussion and technical advices and critical reading of the manuscript.

I would like to express my thanks to Prof. Kiyoshi Sekiguchi and Prof. Masato Okada for review of this thesis.

Finally, I am deeply grateful to my family, my friends, and all members of Laboratory of Regulation of Neuronal Development for their heart-full encouragements, many supports, and kindness.

I thank you, all people and all animals, which gave me good environment and opportunity to research in Dr. Yoshikawa's lab for 6 years.